Journal of Mathematical Modeling
Vol. -, No. -, 2026, pp. -. Research Article

JMM

5-Dimensional intuitionistic fuzzy stochastic multi-objective transportation problem and its solution by evolutionary algorithms

Hardikkumar Radadiya*, Jayesh M. Dhodiya

Department of Mathematics, Sardar Vallabhbhai National Institute of Technology, Surat, Gujarat, India

Email(s): radadiyah45@gmail.com, jdhodiya2002@yahoo.com

Abstract. This paper develops a 5-dimensional intuitionistic fuzzy stochastic multi-objective transportation problem (5DIFSMOTP) model that minimises transportation cost, carbon emissions, labour time, and damage risk. Supply, demand, and conveyance capacity are modelled as stochastic parameters following the logistic distribution, and the penalty coefficients are represented as intuitionistic trapezoidal fuzzy numbers. A new evolutionary algorithm, the Random Loop-based Non-dominated Sorting Evolutionary Algorithm (RLNSEA), is proposed to optimise the transportation flow of the 5DIFSMOTP. The algorithm combines a matrix-based chromosome representation, a feasibility-preserving loop-based update operator, and the NSGA-II selection framework. The proposed algorithm is applied to a case-based numerical illustration of cement transportation across key cities of Gujarat, using hypothetical data. RLNSEA attains a computational time of 573.46 ± 15.23 seconds, which is lower than that of NSGA-II (627.67 ± 18.45 s), NSGA-III (668.56 ± 20.12 s), NSDE-R (619.65 ± 17.89 s), PSO (654.25 ± 19.56 s), and AL-NSGA-III (678.23 ± 21.34 s). The results indicate that RLNSEA is an effective solver for the 5DIFSMOTP within the tested parameter range.

Keywords: 5DIFSMOTP; RLNSEA; fuzzy-stochastic environment; NSGA-II; NSGA-III
AMS Subject Classification 2010: 90B06, 90C29.

1 Introduction

The classical transportation problem (TP), first introduced by Hitchcock [34], involves distributing products from multiple sources to multiple destinations. Traditional TP typically focuses on single-objective optimisation; however, real-world logistics systems require balancing multiple conflicting objectives

*Corresponding author
Received: 29 June 2026/ Revised: 09 November 2026/ Accepted: 11 November 2026
DOI: 10.22124/jmm.2026.34061.3137

© 2026 University of Guilan

Corrected Proof

simultaneously, leading to the development of multi-objective transportation problems (MOTP). The problem has been extended to the solid transportation problem (STP/3DTP), incorporating multiple conveyances, the four-dimensional transportation problem (4DTP), adding alternative routes, and finally the five-dimensional transportation problem (5DTP), which includes drivers as the fifth dimension.

Despite these extensions, existing models have several limitations. Most studies do not account for the importance of drivers, the stochastic nature of supply, demand, and conveyance capacities, and the fuzzy nature of penalty coefficients. Traditional planning models that assume average conditions are no longer adequate in today's uncertain environment. Newer models that incorporate "what-if" scenarios and plan for randomness enable organisations to prepare for uncertainties in advance. Therefore, there is a need for a more comprehensive model that captures both the fuzzy and stochastic nature of the parameters involved in the transportation system. To address these limitations, we propose the 5DIFSMOTP model. This problem considers that products are transported from supply centres to demand centres using different modes of transportation, routes, and drivers. The model incorporates preference weights ϑ_p, predetermined by the decision maker, to reflect the importance of supply centres in optimising transportation flow. Uncertainty in this 5DIFSMOTP is addressed using intuitionistic trapezoidal fuzzy numbers, while uncertainty in supply, demand, and conveyance capacity is addressed using a stochastic environment based on the logistic distribution. The model also considers environmental impact by including carbon emission minimisation as one of the objective functions. Thus, the 5DIFSMOTP model provides a comprehensive representation of transportation problems by incorporating alternative routes, driver skill, and inherent uncertainties in an intuitionistic fuzzy and stochastic environment.

2 Literature review

2.1 Transportation problem dimension

The transportation problem (2DTP) was introduced by Hitchcock [34] and Shell [59], who studied the problem with different transportation modes, called the solid transportation problem (STP) or 3DTP. Bera et al. [12] solved multi-item 4DTP under a budget constraint using rough intervals; Bera et al. [13] solved fixed-charge 4DTP for breakable items under hybrid random type-2 uncertainty; Kakran and Dhodiya [38] solved multi-objective 4DTP in an uncertain environment; Aktar et al. [7] solved 4DTP for breakable incompatible items with type-2 fuzzy random parameters under volume constraints; Bind et al. [14] presented a sustainable multi-objective multi-item 4DTP with triangular intuitionistic fuzzy parameters; Bind et al. [15] proposed a solution strategy for multi-objective green 4DTP under normal type-2 uncertainty; Samanta et al. [57] proposed 4DTP in an intuitionistic LR-type fuzzy environment for minimizing time and maximizing profit.

2.2 The transportation problem in fuzzy-stochastic environment

Zadeh [68] developed fuzzy set theory to model imprecise data via membership functions. Atanas-sov [11] introduced intuitionistic fuzzy sets, adding explicit hesitation to membership and non-membership. Zimmermann [71] proposed fuzzy linear programming for the fuzzy transportation problem (FTP), extended by Abd El-Wahed [1] to single- and multi-objective FTPs. Bit et al. [17] used fuzzy programming (FPT) for MOSTP. Chen et al. [20] proposed entropy-based stochastic parameter transformation with an interior-point method. Giri et al. [32] studied the fuzzy stochastic STP via fuzzy goal programming.

Corrected Proof

Rani and Gulati [53] proposed a compromise method for fully fuzzy multi-objective multi-item STP with trapezoidal fuzzy numbers. Kar et al. [40] considered vehicle cost, volume, and weight capacity under fuzzy chance-constrained programming with credibility theory. Ghosh et al. [30] applied FPT, goal programming, and intuitionistic FPT to fixed-charge MOSTP. Midya et al. [49] presented a multi-stage multi-objective fixed-charge STP in a green supply chain with intuitionistic fuzzy numbers converted via the expected-value operator. Kakran and Dhodiya [38] solved multi-item multi-objective 4DTP using classical methods and LINGO. Devnath et al. [26] formulated a multi-item four-dimensional transportation problem with risk in a fuzzy environment. Samanta et al. [58] proposed a multi-period four-dimensional problem for breakable goods with single-valued neutrosophic parameters, solved by GRG in LINGO-14.0 using possibility measures. Traneva and Tranev [65] proposed an index-matrix interpretation for 3DTP under Elliptic Intuitionistic Fuzzy Quadruples. Dhanapal et al. [27] solved FC4DFTP under a fuzzy-stochastic environment.

Williams [67] presented the stochastic transportation problem via dynamic and nonlinear programming. Cooper and Leblanc [21] developed an algorithm for stochastic transportation and network-type convex problems. Anholcer [9] presented an equalisation algorithm for stochastic generalised transportation with random demand. Acharya et al. [3] solved multi-objective transportation with fuzzy random supplies and demands via alpha-cuts and chance-constrained programming. Roy [56] solved multi-choice stochastic transportation using the Weibull distribution. Singh et al. [60] solved multi-objective STP in a stochastic environment. Agrawal et al. [5] proposed an algorithm for fuzzy fractional stochastic transportation with the exponential distribution. Chaini and Ranarahu [19] proposed a methodology for stochastic transportation with type-2 fuzzy random supply parameters. Abbassi [2] considered uncertainty in objective coefficients and constraint parameters to find robust efficient solutions. Arya et al. [10] solved stochastic STP with Weibull-distributed supply, demand, and conveyance capacity and random cost reduction via fuzzy cost coefficients and alpha-cuts. For the 5DIFSMOTP, literature is limited: Dhanapal et al. [27] solved FC4DFTP in a fuzzy-stochastic environment; Kaspar and Palanivel [42] proposed a robust eco-friendly MOSTP framework; Kapoor et al. [39] proposed an integrated framework for nonlinear multi-objective fully Fermatean-fuzzy stochastic transportation; Rout et al. [55] solved a multi-choice multi-objective fuzzy stochastic transportation problem; Kumar and Mishra [45] solved fuzzy stochastic multi-objective programming; Moges et al. [50] merged goal programming, stochastic optimization, and intuitionistic fuzzy optimization for hierarchical multiobjective fractional stochastic neutrosophic problems; Kumar et al. [46] solved multi-objective neutrosophic fractional stochastic transportation via hesitant fuzzy programming.

2.3 Solution methodologies for multi-objective transportation problems

Early studies used classical optimization, LP, MIP, and GP. Bit et al. [17] applied FPT to MOSTP. Verma et al. [66] applied fuzzy programming with non-linear membership functions. Midya et al. [49] solved deterministic MMFSTP via weighted Tchebycheff and min-max goal programming. Abbassi [2] used weighted sum scalarization for robust efficient solutions. Devnath et al. [26] applied GRG in LINGO under crisp and fuzzy environments. Samanta et al. [58] used possibility measures with GRG in LINGO-14.0 for defuzzification. Das et al. [23] used the ε-constraint approach for cost, customer satisfaction, and sustainable conveyances, comparing it with global criterion, fuzzy programming, and weighted Chebychev programming. Zhang et al. [69] presented a multi-objective evolutionary algorithm for split-delivery vehicle routing with three-dimensional loading. Dhanapal et al. [27] solved FC4DFTP via an improved

Corrected Proof

global weighted sum method. Ali and Javaid [8] developed MOTP and MLMOSTP models with Fermatean fuzzy parameters solved by Fermatean fuzzy programming. Kaspar and Palanivel [42] discussed Neutrosophic Compromise Programming, M-Pareto Optimal, and Neutrosophic Goal Programming for MOSTP. Ding et al. [28] proposed a many-objective multi-population co-evolutionary algorithm. Kapoor et al. [39] proposed an integrated solution for nonlinear multi-objective fully Fermatean-fuzzy stochastic transportation. Moges et al. [50] converted a multi-objective fuzzy stochastic problem into goal programming using intuitionistic fuzzy optimization. Tang et al. [63] developed a reinforcement-learning-assisted hybrid evolutionary framework. Zhang et al. [70] solved high-dimensional multimodal multi-objective optimization via subspace projection and angular diversity. Evolutionary algorithms (EAs) such as genetic algorithms (GA) and evolutionary strategies (ES) are increasingly popular. GAs were introduced by Holland [35]. Multi-objective variants include NSGA by Srinivas et al. [62], NSGA-II by Deb et al. [24], NSGA-III by Jain et al. [36], NSDE-R by Reddy et al. [54], PSO by Kennedy et al. [44], and AL-NSGA-III by Todkar and Dhodiya [64], all of which approximate Pareto fronts without preference specification. Other recent EAs (Tang et al. [63], Ding et al. [28], Zhang et al. [69], Zhang et al. [70]) are generic and do not exploit problem structure. Accordingly, the 5DIFSMOTP in this paper is addressed using standard evolutionary algorithms (NSGA-II/III, NSDE-R, PSO, and AL-NSGA-III).

2.4 Research gap

The study of higher-dimensional transportation problems remains limited. Dhanapal et al. [27] solved a 4-dimensional problem but did not incorporate the stochastic nature of supply and demand, while Kumar & Singh [46] addressed stochasticity but not the higher-dimensional case. Table 1 shows that no existing work combines a 5-dimensional transportation problem with intuitionistic fuzzy stochastic uncertainty and multiple conflicting objectives. Two gaps persist: (i) no integration of stochastic supply, demand, and conveyance capacity in a 5-dimensional setting, and (ii) limited application of advanced evolutionary algorithms to 5-dimensional transportation, because classical methods struggle with high dimensionality, and the need to generate multiple Pareto-optimal solutions in a single run, while evolutionary algorithms require careful parameter tuning, feasible initial population generation, and considerable computational effort.

2.5 Contribution and novelty

This study makes the following contributions:

- A 5-dimensional stochastic transportation model: The five dimensions (sources, destinations, conveyances, routes, drivers) are integrated with stochastic supply, demand, and conveyance capacity, providing a formulation for transportation flow allocation under uncertainty.
- Intuitionistic trapezoidal fuzzy parameter modelling: Cost, carbon emissions, labour time, and damage risk are treated as intuitionistic trapezoidal fuzzy numbers, and the hybrid uncertain model is transformed into a deterministic equivalent.
- A multi-objective framework with conflicting objectives: The model simultaneously minimises cost, carbon emissions, labour time, and damage risk, providing a set of Pareto-optimal trade-off solutions to the decision-maker.
- A feasibility-preserving evolutionary algorithm (RLNSEA): The algorithm incorporates a matrix-based feasible initial population and a feasibility-preserving loop mutation, so that all generated solu-

Corrected Proof

Table 1: Literature review: Multi-objective transportation problem

References	Dimensions	Objective	Uncertainty	Solution method
Kaushal et al. [43]	4	Single	✓	Standard LP
Midya et al. [49]	3	Multi	✓	WTM
Ghosh et al. [31]	3	Multi	×	NLP, FP, GCM
Mondal et al. [51]	3	Multi	×	NSGA
Devnath et al. [26]	4	Single	✓	GRG
Buvaneshwari & Anuradha [18]	3	Multi	×	GWSM
Aktar et al. [7]	4	Multi	×	WSM, NLP, MMM
C. Kar et al. [41]	4	Single	×	GRG
Samanta et al. [58]	4	Single	✓	GRG
Das et al. [23]	3	Multi	✓	ε-C, WCP
Traneva & Tranev [65]	3	Single	✓	IMA
Ali & Javaid [8]	3	Multi	✓	FFP
Kaspar & Palanivel [42]	3	Multi	✓	NCP
Dhanapal et al. [27]	4	Multi	✓	EGWSM
Kapoor et al. [39]	2	Multi	✓	FFP
Rout et al. [55]	2	Multi	✓	FP
Moges et al. [50]	2	Multi	✓	GP
Kumar & Mishra [45]	2	Multi	✓	GP
Kumar & Singh [46]	2	Multi	✓	HMS
Present article	5	Multi	✓	NSGA-III (best), NSGA-II, NSDE-R, PSO, AL-NSGA-III

Abbreviations: LP: linear programming; WTM: weighted Tchebycheff metrics; NLP: neutrosophic linear programming; FP: fuzzy programming; GCM: global criterion method; NSGA: non-dominated sorting genetic algorithm; GRG: generalized reduced gradient; GWSM: global weighted sum method; WSM: weighted sum method; MMM: max-min method; ε-C: ε-constraint; WCP: weighted Chebychev programming; IMA: index-matrix based algorithm; FFP: Fermatean fuzzy programming; NCP: neutrosophic compromise programming; EGWSM: enhanced global weighted sum method; GP: goal programming; HMS: hybrid multi-stage.

tions satisfy the constraints by construction.

- A case-based numerical illustration: The model is applied to a case-based illustration of cement transportation across key cities of Gujarat using hypothetical data.
- Comparative benchmarking: RLNSEA is benchmarked against NSGA-II, NSGA-III, NSDE-R, PSO, and AL-NSGA-III, and the comparison is supported by five performance indicators, feasibility and coverage analyses, and the Wilcoxon and Friedman tests.

2.6 Mathematical formulation of 5DIFSMOTP

Consider a logistics network in which the commodity is transported from a set of supply centres to a set of final demand centres. The transportation system has five dimensions: the supply centres (origins), the demand centres (destination), the type of conveyance (vehicle mode), the route taken between locations, and the driver skill level. All these dimensions affect costs, emissions, labour time, and the risk of damage.

2.7 Notation

To formulate the 5DIFSMOTP, we define the sets, parameters, and decision variables in Table 2.

Corrected Proof

Table 2: Notation used in the 5DIFSMOTP model

Symbol	Description
Sets and indices	
P, Q, R, S, T, E	Sets of sources, destinations, conveyances, routes, drivers, and commodity types, with cardinalities u, v, w, l, m, h
Parameters	
s_p, d_q, n_r	Supply at source p, demand at destination q, and maximum capacity of conveyance r
ϑ_p	Decision-maker's weight for supply centre p, with $\sum_{p=1}^{u} \vartheta_p = 1$, $\vartheta_p \geq 0$
$\tilde{c}_{pqrste}$, $\tilde{f}_{pqrste}$, $\tilde{\tau}_{pqrste}$, $\tilde{g}_{pqrste}$	transportation cost, carbon emission, labour time, and damage risk in TrIF environment; c_{pqrste}, f_{pqrste}, τ_{pqrste}, g_{pqrste} are the corresponding crisp values
α_p, β_p	Location and scale parameters of the logistic distribution for supply s_p
γ_q, δ_q	Location and scale parameters of the logistic distribution for demand d_q
ϕ_r, λ_r	Location and scale parameters of the logistic distribution for conveyance capacity n_r
$\theta_p, \varepsilon_q, \mu_r$	Allowed violation probabilities for the supply, demand, and conveyance-capacity constraints, each in $(0,1)$; the corresponding reliability levels are $1-\theta_p$, $1-\varepsilon_q$, and $1-\mu_r$.
$\tilde{s}(\theta_p), \tilde{d}(\varepsilon_q), \tilde{n}(\mu_r)$	Stochastic supply at allowed violation probability θ_p stochastic demand at allowed violation probability ε_q, and stochastic conveyance capacity at μ_r.
π_d, κ	Mean of paired differences between two algorithms; significance level (typically $\kappa = 0.05$)
Decision variable	
x_{pqrste}	Quantity shipped from source p to destination q by conveyance r on route s with driver t for commodity e; $x_{pqrste} \geq 0$
Objective functions	
$\tilde{Z}_1, \tilde{Z}_2, \tilde{Z}_3, \tilde{Z}_4$	Total weighted cost (rupees), weighted carbon emissions (kg), weighted labour time (minutes), and weighted damage risk (scale 1 to 5) in TrIF environment; Z_1 to Z_4 are the corresponding crisp values and we simply refer Total weighted transportation cost as total transportation cost, similarly, for weighted carbon emission, weighted labour time, and weighted damage risk.

2.8 5DIFSMOTP optimization model

Model 1 represents the five-dimensional multi-objective transportation problem, formulated to optimize multiple conflicting objectives. The model considers transportation from sources to destinations. It incorporates four objective functions: Z_1 minimizes the total transportation cost; Z_2 minimizes the total carbon-dioxide emissions; Z_3 minimizes the total labour time associated with loading and unloading; and Z_4 minimizes the risk of damage during transportation. These objectives are subject to supply, demand, and conveyance capacity constraints that ensure the system's feasibility.

Model-1

Objective Functions:

$$\min Z_1 = \sum_{p=1}^{u}\sum_{q=1}^{v}\sum_{r=1}^{w}\sum_{s=1}^{l}\sum_{t=1}^{m}\sum_{e=1}^{h} \vartheta_p c_{pqrste} x_{pqrste}; \tag{1}$$

$$\min Z_2 = \sum_{p=1}^{u}\sum_{q=1}^{v}\sum_{r=1}^{w}\sum_{s=1}^{l}\sum_{t=1}^{m}\sum_{e=1}^{h} \vartheta_p f_{pqrste} x_{pqrste}; \tag{2}$$

$$\min Z_3 = \sum_{p=1}^{u}\sum_{q=1}^{v}\sum_{r=1}^{w}\sum_{s=1}^{l}\sum_{t=1}^{m}\sum_{e=1}^{h} \vartheta_p \tau_{pqrste} x_{pqrste}; \tag{3}$$

$$\min Z_4 = \sum_{p=1}^{u}\sum_{q=1}^{v}\sum_{r=1}^{w}\sum_{s=1}^{l}\sum_{t=1}^{m}\sum_{e=1}^{h} \vartheta_p g_{pqrste} x_{pqrste}; \tag{4}$$

Subject to the constraints:

Corrected Proof

$$\sum_{q=1}^{v}\sum_{r=1}^{w}\sum_{s=1}^{l}\sum_{t=1}^{m}\sum_{e=1}^{h} x_{pqrste} \le s_p, \quad \forall p; \tag{5}$$

$$\sum_{p=1}^{u}\sum_{r=1}^{w}\sum_{s=1}^{l}\sum_{t=1}^{m}\sum_{e=1}^{h} x_{pqrste} \ge d_q, \quad \forall q; \tag{6}$$

$$\sum_{p=1}^{u}\sum_{q=1}^{v}\sum_{s=1}^{l}\sum_{t=1}^{m}\sum_{e=1}^{h} x_{pqrste} \le n_r, \quad \forall r; \tag{7}$$

$$x_{pqrste} \ge 0, \quad \forall p,q,r,s,t,e. \tag{8}$$

It is evident that model-1 provides a feasible solution if

$$\sum_{\forall p} s_p \ge \sum_{\forall q} d_q \quad \& \quad \sum_{\forall r} n_r \ge \sum_{\forall q} d_q. \tag{9}$$

In model-1, the first constraint (5) imposes a restriction on the transportation of goods to ensure the availability of the sources, and constraint (6) ensures that the demand for goods required by customers at the destination is met. The constraints (7) give the capacity of the conveyances. Constraints (8) and (9) ensure the feasibility and non-negativity of the decision variables. In model-1, the variables s_p, d_q, n_r, c_{pqrste}, f_{pqrste}, τ_{pqrste}, and g_{pqrste} are related to supply, demand, conveyance capacity, transportation cost, carbon emission, delivery time, and damage risk, respectively. However, in practical situations, it is very difficult to determine the exact values of these parameters due to their inherent vagueness. In this case, if we consider the 5DMOTP parameters to be fuzzy and stochastic, this is closer to reality, as represented in model 2. The weights ϑ_p, which sum to 1, represent the decision-maker's relative importance attached to each supply centre. Consequently, the objective functions Z_1 to Z_4 are weighted performance measures rather than physical totals; the physical totals are recovered by setting all weights equal to 1. This model has six indices p, q, r, s, t, and e, but when the commodity is fixed to one item, i.e. $e = 1$, the model becomes five-dimensional.

Model-2

The Model of 5-dimensional stochastic multi-objective transportation with intuitionistic fuzzy numbers is given as follows:

$$\min \tilde{Z}_1 = \sum_{p=1}^{u}\sum_{q=1}^{v}\sum_{r=1}^{w}\sum_{s=1}^{l}\sum_{t=1}^{m}\sum_{e=1}^{h} \vartheta_p \tilde{c}_{pqrste} x_{pqrste}; \tag{10}$$

$$\min \tilde{Z}_2 = \sum_{p=1}^{u}\sum_{q=1}^{v}\sum_{r=1}^{w}\sum_{s=1}^{l}\sum_{t=1}^{m}\sum_{e=1}^{h} \vartheta_p \tilde{f}_{pqrste} x_{pqrste}; \tag{11}$$

$$\min \tilde{Z}_3 = \sum_{p=1}^{u}\sum_{q=1}^{v}\sum_{r=1}^{w}\sum_{s=1}^{l}\sum_{t=1}^{m}\sum_{e=1}^{h} \vartheta_p \tilde{\tau}_{pqrste} x_{pqrste}; \tag{12}$$

$$\min \tilde{Z}_4 = \sum_{p=1}^{u}\sum_{q=1}^{v}\sum_{r=1}^{w}\sum_{s=1}^{l}\sum_{t=1}^{m}\sum_{e=1}^{h} \vartheta_p \tilde{g}_{pqrste} x_{pqrste}; \tag{13}$$

Subject to the constraints:

$$\Pr\left(\sum_{q=1}^{v}\sum_{r=1}^{w}\sum_{s=1}^{l}\sum_{t=1}^{m}\sum_{e=1}^{h} x_{pqrste} \le s_p\right) \ge 1-\theta_p, \quad \forall p; \tag{14}$$

$$\Pr\left(\sum_{p=1}^{u}\sum_{r=1}^{w}\sum_{s=1}^{l}\sum_{t=1}^{m}\sum_{e=1}^{h} x_{pqrste} \ge d_q\right) \ge 1-\varepsilon_q, \forall q; \tag{15}$$

$$\Pr\left(\sum_{p=1}^{u}\sum_{q=1}^{v}\sum_{s=1}^{l}\sum_{t=1}^{m}\sum_{e=1}^{h} x_{pqrste} \le n_r\right) \ge 1-\mu_r, \quad \forall r; \tag{16}$$

$$x_{pqrste} \ge 0 \quad \forall p,q,r,s,t,e.$$

Corrected Proof

Where, θ_p, ε_q, and μ_r are allowed violation probabilities; $1-\theta_p$, $1-\varepsilon_q$, and $1-\mu_r$ are the corresponding reliability levels. Increasing θ_p from 0.1 to 0.9 makes the supply constraint less conservative. Let $\tilde{s}(\theta_p)$, $\tilde{d}(\varepsilon_q)$ and $\tilde{n}(\mu_r)$ are stochastic supply, demand, and conveyance capacity corresponding to equations-(14), (15) and (16), then the feasibility requires aggregate conditions to hold: (i) $\sum_p \tilde{s}_p \geq \sum_q \tilde{d}_q$, means total stochastic supply is sufficient to meet total stochastic demand; (ii) $\sum_r \tilde{n}_r \geq \sum_q \tilde{d}_q$, means stochastic conveyance capacity is sufficient to carry the total stochastic demand; and the confidence ranges depends on problem specific instances, for which the stochastic supply at the lowest supply reliability exceeds the nominal demand and nominal supply exceeds the stochastic demand at the highest demand reliability for that range, similarly for conveyance capacity and demand(The term nominal used to distinguish the fixed baseline values(given in Tables-3(a), 3(b), and 3(c), in Section 6 in Supplementary document) from the experimentally varied values). The chance constraints are imposed individually for supply, demand, and conveyance means when supply varies, demand is taken as fixed, similarly for demand, and conveyance capacity for conditions (i) and (ii). In case-based illustration, conditions (i) and (ii) hold; further details are given in the case-based illustration section. The reliability levels specified in this study apply to the individual stochastic constraints, each imposed separately. They do not, by themselves, establish the same reliability level for the joint event that all stochastic constraints hold simultaneously. For the reliability levels used in this case-based illustration study, the joint event is verified numerically (see the margins reported in Section 6), but this verification is instance-specific and does not provide a general joint-chance guarantee; at other levels, the joint event may fail, and in that case no feasible solution exists.

In the intuitionistic fuzzy set theory, the Trapezoidal intuitionistic fuzzy numbers (TrIFNs) are used to model parameters that are uncertain or imprecise by specifying both a membership degree, which expresses confidence that the true value lies within a most plausible range, and a non-membership degree, which expresses confidence that it lies outside that range, together with a hesitancy degree that captures the remaining uncertainty; in transportation optimization they allow cost, emissions, labour time, and damage risk to be represented more realistically than crisp numbers, because the decision maker can encode not only the likely interval of each parameter but also how much confidence or doubt to place in that interval, and these intuitionistic fuzzy coefficients can then be defuzzified into crisp values. For further details on intuitionistic fuzzy set theory, the reader is referred to the cited references. For example, a cost coefficient with a narrow interval of full membership and a narrow interval of full non-membership indicates a parameter that is well understood, whereas wide intervals indicate a parameter subject to substantial uncertainty. The following theorem provides a closed-form expression for the expected value (EV) of a Trapezoidal intuitionistic fuzzy number (TrIF number) [52] [33] [11].

Theorem 1. *Let* $\tilde{A} = \langle(\zeta_1,\zeta_2,\zeta_3,\zeta_4),(\nu_1,\nu_2,\nu_3,\nu_4)\rangle$ *be a TrIF number. Its expected value is* $\mathrm{EV}(\tilde{A}) = \frac{1}{8}\sum_{i=1}^{4}(\zeta_i+\nu_i)$. *If* $\zeta_i = \nu_i$ *for all i, then* $\mathrm{EV}(\tilde{A}) = \frac{1}{4}\sum_{i=1}^{4}\zeta_i$.

Proof. It follows directly from the framework for the expected interval and expected value of intuitionistic fuzzy numbers established by Grzegorzewski [33]. Therefore, it is omitted. □

Using Theorem 1, the TrIF objectives in (1), (2), (3), and(4) are converted to crisp form. For example,

$$\min \tilde{Z}_1 = \sum_{p,q,r,s,t,e} \vartheta_p \langle (c^1_{pqrste},\ldots,c^4_{pqrste}),(c'^1_{pqrste},\ldots,c'^4_{pqrste})\rangle x_{pqrste},$$

Corrected Proof

with

$$c_{pqrste} = \mathrm{EV}(\tilde{c}_{pqrste}) = \frac{1}{8}\sum_{k=1}^{4}\left(c^{k}_{pqrste} + c'^{k}_{pqrste}\right).$$

The coefficients for carbon emissions, labour time, and damage risk are obtained in a similar manner. The logistic distribution is adopted in this study for two reasons. First, it is a standard choice in the stochastic transportation literature, where it has been used for supply and demand parameters by Agrawal and Ganesh (2018) [4], Mahapatra et al. (2020) [48], Gessesse and Mishra (2021) [29], and Biswas et al. (2026) [16]. Second, the logistic distribution stands out for our convenience in solving the problem for three key reasons. First, its heavier tails provide a more realistic representation of extreme deviations observed in transportation systems compared to the normal distribution. Second, it offers a closed-form quantile function, given by $F^{-1}(y) = \alpha + \beta \ln(y/(1-y))$, which enables a direct and computationally efficient transformation of probabilistic chance constraints into deterministic linear constraints without relying on numerical integration or iterative solvers, which is a crucial advantage for large-scale multi-objective optimization. Third, its location-scale parametrization (α_p and β_p) offers an intuitive interpretation of shifts and dispersions in supply, demand, and capacity parameters, which aligns seamlessly with the physical meaning of these quantities in our model. The choice of a probability distribution for modelling stochastic parameters is inherently problem-dependent; no single distribution universally outperforms all others. In our specific framework, the 5DIFSMOTP, the logistic distribution is adopted because it aligns particularly well with the empirical nature of transportation uncertainties and the mathematical requirements of our solution strategy. However, we emphasize that practitioners are free to select alternative distributions (e.g., normal, Weibull, lognormal, Laplace, or Student's t) depending on the actual data characteristics and modelling objectives of their own problems. The 5DIFSMOTP have two types of uncertainty. Constraints of the 5DIFSMOTP are stochastic in form, which is to be converted into deterministic form using the article of [[4], [61]]. The second is intuitionistic fuzzy (in TrIF) uncertainty, which is converted to a deterministic form by the expected value operator to defuzzify the fuzzy objective coefficients. The membership and non-membership functions, along with the defuzzification/expected-value operator for intuitionistic trapezoidal fuzzy numbers, are detailed in the cited documents. These functions convert fuzzy cost, emission, time, and risk coefficients into crisp values. Specifically, the membership function $\mu_{\tilde{A}}(x)$ and non-membership function $\nu_{\tilde{A}}(x)$ for an intuitionistic trapezoidal fuzzy number $\tilde{A} = (a_1, a_2, a_3, a_4; a'_1, a'_2, a'_3, a'_4)$ are defined in the preliminaries section. The expected value operator for defuzzification is applied to obtain crisp equivalents of the fuzzy objective coefficients. These crisp values are then used in the deterministic Model-2. We consider supply, demand, and conveyance capacity to be stochastic; let them follow a logistic distribution. If α and β are the location and scale parameters for a random variable x, then the probability density function of the logistic distribution is represented as follows:

$$f(x,\alpha,\beta) = \frac{1}{\beta}\frac{e^{-\frac{x-\alpha}{\beta}}}{\left(1+e^{-\frac{x-\alpha}{\beta}}\right)^2}, \quad F(x) = \frac{1}{1+e^{-\frac{x-\alpha}{\beta}}}, \quad F^{-1}(y) = \alpha + \beta \ln\left(\frac{y}{1-y}\right).$$

Let $S_p = \sum_{q,r,s,t,e} x_{pqrste}$, $D_q = \sum_{p,r,s,t,e} x_{pqrste}$, $N_r = \sum_{p,q,s,t,e} x_{pqrste}$. the probabilistic constraints becomes,

$$\Pr(s_p \geq S_p) \geq 1-\theta_p \implies S_p \leq \alpha_p + \beta_p \ln\left(\frac{\theta_p}{1-\theta_p}\right),$$

Corrected Proof

$$\Pr(d_q \le D_q) \ge 1-\varepsilon_q \implies D_q \ge \gamma_q + \delta_q \ln\left(\frac{1-\varepsilon_q}{\varepsilon_q}\right),$$
$$\Pr(n_r \ge N_r) \ge 1-\mu_r \implies N_r \le \phi_r + \lambda_r \ln\left(\frac{\mu_r}{1-\mu_r}\right).$$

After converting the fuzzy and stochastic uncertainty into a deterministic form, the model becomes:
Model-3:

$$\min Z_1 = \sum_{p=1}^{u}\sum_{q=1}^{v}\sum_{r=1}^{w}\sum_{s=1}^{l}\sum_{t=1}^{m}\sum_{e=1}^{h} \vartheta_p c_{pqrste} x_{pqrste}; \tag{17}$$

$$\min Z_2 = \sum_{p=1}^{u}\sum_{q=1}^{v}\sum_{r=1}^{w}\sum_{s=1}^{l}\sum_{t=1}^{m}\sum_{e=1}^{h} \vartheta_p f_{pqrste} x_{pqrste}; \tag{18}$$

$$\min Z_3 = \sum_{p=1}^{u}\sum_{q=1}^{v}\sum_{r=1}^{w}\sum_{s=1}^{l}\sum_{t=1}^{m}\sum_{e=1}^{h} \vartheta_p \tau_{pqrste} x_{pqrste}; \tag{19}$$

$$\min Z_4 = \sum_{p=1}^{u}\sum_{q=1}^{v}\sum_{r=1}^{w}\sum_{s=1}^{l}\sum_{t=1}^{m}\sum_{e=1}^{h} \vartheta_p g_{pqrste} x_{pqrste}; \tag{20}$$

Subject to the constraints:

$$\sum_{q=1}^{v}\sum_{r=1}^{w}\sum_{s=1}^{l}\sum_{t=1}^{m}\sum_{e=1}^{h} x_{pqrste} \le \alpha_p + \beta_p \ln\left(\frac{\theta_p}{1-\theta_p}\right), \forall p \tag{21}$$

$$\sum_{p=1}^{u}\sum_{r=1}^{w}\sum_{s=1}^{l}\sum_{t=1}^{m}\sum_{e=1}^{h} x_{pqrste} \ge \gamma_q + \delta_q \ln\left(\frac{1-\varepsilon_q}{\varepsilon_q}\right), \forall q \tag{22}$$

$$\sum_{p=1}^{u}\sum_{q=1}^{v}\sum_{s=1}^{l}\sum_{t=1}^{m}\sum_{e=1}^{h} x_{pqrste} \le \phi_r + \lambda_r \ln\left(\frac{\mu_r}{1-\mu_r}\right), \forall r \tag{23}$$

$$x_{pqrste} \ge 0, \quad \forall p,q,r,s,t,e. \tag{24}$$

Where α_p, β_p, and θ_p are location and scale parameters, and the allowed violation probability associated with the p-th supply centre; γ_q, δ_q, and ε_q correspond to the demand of customers; and ϕ_r, λ_r, and μ_r correspond to the conveyance capacity of transportation, respectively. In our framework, the DM is required to fix the allowed violation probabilities θ_p, ε_q, and μ_r a priori. Once these allowed violation probabilities are specified, the chance constraints are transformed into their deterministic equivalents using the logistic distribution (as given in Equations (21), (22), and (23)) in order to solve 5DIFSMOTP.

3 Solution methodology

The RLNSEA algorithm is specifically designed to preserve the feasibility of solutions throughout the entire optimization process. Unlike traditional evolutionary algorithms that rely on penalty functions or repair mechanisms to handle constraint violations, RLNSEA ensures feasibility by mathematical construction at every stage of the algorithm. The RLNSEA adopts the standard components from NSGA-II: non-dominated sorting for ranking solutions, crowding-distance calculation for maintaining diversity, and tournament selection for choosing promising solutions. These components are well-established and widely used in multi-objective evolutionary algorithms. They serve as the backbone of our algorithm because of their proven effectiveness in handling multi-objective optimization problems. The novelty of RLNSEA lies not in these standard mechanisms, but in the following problem-specific components that fundamentally change how solutions are represented, generated, and improved.

Corrected Proof

3.1 Random loop-based non-dominated sorting evolutionary algorithm

The RLNSEA is a novel problem-specific extension of the NSGA-II framework for solving higher-dimensional multi-objective transportation problems. While it retains the standard non-dominated sorting, crowding distance, and tournament selection mechanisms from NSGA-II, it introduces three key novel components: (i) a matrix-based chromosome representation that captures the multi-dimensional structure of the problem, (ii) the use of random loops, rather than deterministic pivots, as the offspring-generating mechanism inside a multi-objective evolutionary algorithm, and (iii) a feasibility-preserving mechanism that guarantees all generated solutions are strictly feasible without requiring repair or penalty functions. These modifications constitute a significant algorithmic innovation for this specific problem class, achieving statistically higher performance than general-purpose algorithms while preserving the proven effectiveness of NSGA-II's selection framework.

3.2 Steps of RLNSEA for the 5DIFSMOTP

Step 1 Problem setup: Consider the 5DIFSMOTP and determine its supply, demand, and conveyance capacity constraints, together with the objective functions.

Step 2 Matrix-based initialization: A population of chromosomes is constructed by a matrix-based approach adapted from Agnihotri & Dhodiya [6], who introduced a matrix-based population for the multi-objective solid transportation problem. The same fundamental principle is applied here to the 5DIFSMOTP and extended to the five-dimensional setting, as described in Algorithm 1 in subsection 3.1 of the Supplementary document. The initialisation procedure constructs a feasible solution for the deterministic model, which satisfies two aggregate conditions: (i) total supply is at least total demand, $\sum_p s_p \geq \sum_q d_q$; (ii) total conveyance capacity is at least total demand, $\sum_r n_r \geq \sum_q d_q$; since $\sum_p s_p \geq \sum_q d_q$ and $\sum_r n_r \geq \sum_q d_q$, satisfies in the considered case-based illustration with specified reliability levels, to generate initial population it is sufficient to satisfy only supply, demand, and conveyance capacity constraints, a mechanism to produce initial population is given in algorithm 1 given in subsection 3.1 in the Supplementary document; For case-based illustration, the confidence levels are chosen so that the effective supply at the lowest supply reliability exceeds the nominal effective demand, and the nominal effective supply exceeds the effective demand at the highest demand reliability. These conditions guarantee feasibility of the deterministic model used by the algorithm; they do not, by themselves, guarantee that the original stochastic system satisfies all constraints simultaneously at any reliability levels.
The feasibility guarantee established by Algorithm 1 (given in Subsection 3.1 in the Supplementary document) pertains exclusively to the specified reliability of the deterministic model. When demand, supply availability or conveyance capacity are random, the quantities $\sum_{\forall p} \tilde{s}_p$, $\sum_{\forall q} \tilde{d}_q$, and $\sum_{\forall r} \tilde{n}_r$ are themselves random variables, so the inequalities $\sum_p \tilde{s}_p \geq \sum_q \tilde{d}_q$ and $\sum_r \tilde{n}_r \geq \sum_q \tilde{d}_q$ may hold for the specific reliability levels used in the deterministic model while failing for other reliability levels.

At each visited cell (p,q,r,s,t,e), the allocated quantity is

$$a_{pqrste} = \min\left(s_p^{\text{rem}},\, d_q^{\text{rem}},\, n_r^{\text{rem}}\right),$$

and the three residuals are decremented by this amount. Because the allocation never exceeds any of the three residuals, no supply, demand, or conveyance constraint is violated at any step, since $\sum_p s_p \geq \sum_q d_q$ and $\sum_r n_r \geq \sum_q d_q$ are satisfied in the deterministic model; so to generate the initial population, thus the resulting chromosome A is feasible by construction. The extension of the original MOSTP scheme

Corrected Proof

to the 5DIFSMOTP consists of (i) iterating over the full five-dimensional index set (p,q,r,s,t), and (ii) incorporating the conveyance capacity as a third residual alongside supply and demand. The fundamental principle of allocating the minimum of the remaining capacities at each step is preserved.

Step 3 Loop-based update matrix: To improve the feasible population, a loop-based update matrix $X = (x_{pqrste})$ is generated, satisfying

$$\sum_{q,r,s,t,e} x_{pqrste} = 0 \ \forall p, \qquad \sum_{p,r,s,t,e} x_{pqrste} = 0 \ \forall q, \qquad \sum_{p,q,s,t,e} x_{pqrste} = 0 \ \forall r,$$

and

$$x_{pqrste} \in \{1,0,-1\} \quad \forall p,q,r,s,t,e.$$

The zero-sum conditions ensure that the update only redistributes flow between positions without changing row, column, or conveyance totals, and the entries in $\{1,0,-1\}$ preserve the feasibility of the updated chromosome.

Step 4 Feasibility-preserving update: Let

$$S = \{a_{pqrste} \mid x_{pqrste} < 0\}$$

be the set of entries of the current feasible solution A at positions where the update matrix is negative, and let $\min(S)$ be the smallest such entry. The updated chromosome is

$$(n_{pqrste}) = (a_{pqrste}) + \eta\,(x_{pqrste}), \qquad \eta \in [0, \min(S)].$$

Because the reduction (when $x_{pqrste} = -1$) never exceeds a_{pqrste}, the updated chromosome satisfies $n_{pqrste} \geq 0$. The interval $[0, \min(S)]$ is the feasible range for η; any value within this range preserves feasibility, and a random value is chosen to promote diversity. Unlike classical genetic algorithms that rely on crossover and mutation with repair operators, RLNSEA uses a single loop-based update that is feasibility-preserving by construction, so no repair mechanism is required. The feasibility of the updated solution is mathematically guaranteed by the constraints given below:
Supply Constraints:

$$\sum_{q,r,s,t,e} n_{pqrste} = \sum_{q,r,s,t,e} a_{pqrste} + \eta \sum_{q,r,s,t,e} x_{pqrste} \leq s_p + 0 = s_p.$$

Similarly, the updated solution satisfies the feasibility constraints for demand and conveyance.

Step 5 Population update: Repeat Step 4 to generate a new population by updating the initial population.

Step 6 Merging and non-dominated sorting: Let $\{X^k\}_{k=1}^{n}$ be the initial population and $\{Y^k\}_{k=1}^{m}$ the newly generated population, with $1 \leq m \leq n$. The merged set is

$$Z = \Big(\bigcup_{k=1}^{n} X^k\Big) \cup \Big(\bigcup_{k=1}^{m} Y^k\Big).$$

Evaluate the fitness of each element of Z and apply non-dominated sorting [25]. A solution x dominates a solution y if $Z_k(x) \leq Z_k(y)$ for all k and $Z_k(x) < Z_k(y)$ for at least one k. The first non-dominated front

Corrected Proof

F_1 consists of solutions with domination count zero. Solutions in F_1 are assigned rank 1, those in F_2 rank 2, and so on. The crowding distance of the j-th solution in the sorted list for the m-th objective is

$$d(I_j^m) = d(I_j^m) + \frac{f_m(I_{j+1}^m) - f_m(I_{j-1}^m)}{f_m^{\max} - f_m^{\min}},$$

with the boundary solutions assigned an infinite crowding distance.

Step 7 Crowding-distance tournament selection: A solution x wins the crowding-distance tournament over y if either $r_x < r_y$, or $r_x = r_y$ and $d_x > d_y$, where r and d denote the rank and crowding distance. Binary tournament selection is applied using this criterion. From the $2N$ solutions in the merged set, N solutions are selected to form the next generation.

Step 8 Termination: Repeat Steps 2-7 until efficient non-dominated solutions are obtained. If the non-dominated set remains unchanged as the population size and number of generations increase, the solutions are considered efficient. The pseudocode for implementing the proposed RLNSEA for optimising multi-objectives and generating Pareto fronts is presented in Algorithms 1, 2, and 3 in Section 3 of the Supplementary document. These pseudocode snippets provide a clear and reproducible view of the computational processes used in the numerical experiment.

4 A case-based illustration: The transportation of cement from industries

The case-based illustration is given in this section. It is a numerical demonstration based on hypothetical data and does not constitute empirical validation against any cement industry's historical transportation records. The purpose is to illustrate how the proposed framework operates under a realistic transportation setting, not to establish that the reported numerical values would be reproduced in an actual logistics operation. In Gujarat, major cities such as Bhuj, Rajkot, Bhavnagar, Ahmedabad, and Surat host several cement industries that play a vital role in the state's construction and infrastructure development. The cement produced in these industrial hubs is transported to 5 fixed destinations. The study is described as a case-based illustration (hypothetical data) of cement transportation across key cities in Gujarat, organised by geography and scale; the locations and capacities are hypothetical and not drawn from measured industry records. In this case-based illustration, the data on supply, demand, and conveyance capacity are given in Table 3 in Section 6 in the supplementary document, with the locations of the supply and demand centres, and corresponding weights are provided in Table 8 in Section 7 of the Supplementary document. The weights ϑ_p assigned to the five supply centres are taken proportional to their supply capacity:

$$\vartheta_p = \frac{s_p}{\sum_{p'=1}^{5} s_{p'}}, \qquad p = 1, 2, \ldots, 5.$$

With $\sum_{p=1}^{5} s_p = 6500$, this gives $\vartheta_1 = 0.1662$, $\vartheta_2 = 0.1877$, $\vartheta_3 = 0.2492$, $\vartheta_4 = 0.2000$, and $\vartheta_5 = 0.1969$, normalised so that $\sum_{p=1}^{5} \vartheta_p = 1$.

The stochastic nature of supply, demand, and conveyance capacities arises from uncertainty in industrial production capacity. Customers may increase or decrease demand based on their circumstances and needs; the conveyance capacity also varies due to maintenance-related issues. This stochastic nature is addressed by the decision maker(DM) utilizing a logistic distribution with predetermined allowed violation probabilities. Each city has a fixed number of labourers hired at a fixed hourly rate. After reaching

Corrected Proof

the supply centre, the conveyances queue up in front of the centre. Once the cement bags are loaded, the conveyance is driven by one of two drivers along one of two routes to the customers (destinations). The route and driver are chosen based on their suitability for the road conditions, traffic, weather, and potential hazards, as determined by the DM. The demand centres are specified by the optimal schedule decided by the DM, who selects solutions based on Pareto optimality. Upon arrival at the demand centre, the truck is unloaded by labourers hired by the demand centre owners. It notes that supply, demand, and conveyance capacity are quantified in terms of the number of cement bags; each bag contains 50 kg of cement, so the decision variable represents the number of bags to be transported rather than the direct quantity of cement. Transportation costs, carbon emissions, and labour time are proportional to the distances between supply centres and demand centres (destinations). Data on the distances between supply and demand centres across two routes are provided in Table 8 in Section 7 of the Supplementary document. While damage risk has a conflicting nature with transportation cost, if customers want low damage risk, then its corresponding transportation cost will be high, as it requires proper care, low speed, which increases transportation time, and the driver will charge more; all of these four objectives are considered in an intuitionistic fuzzy environment by using trapezoidal intuitionistic fuzzy numbers to address uncertainty. The conflict between transportation costs and damage risk is inherent in the damage-risk data; note that the data used in the study of cement transportation are hypothetical. Data on transportation costs, loading and unloading times, carbon emissions, and transportation damage risk require extensive space, so they are provided in a DOI provided in the data availability subsection. Damage risk is quantified on a scale of 1 to 5, where 1 is very low, 2 is low, 3 is medium, 4 is high, and 5 is very high.

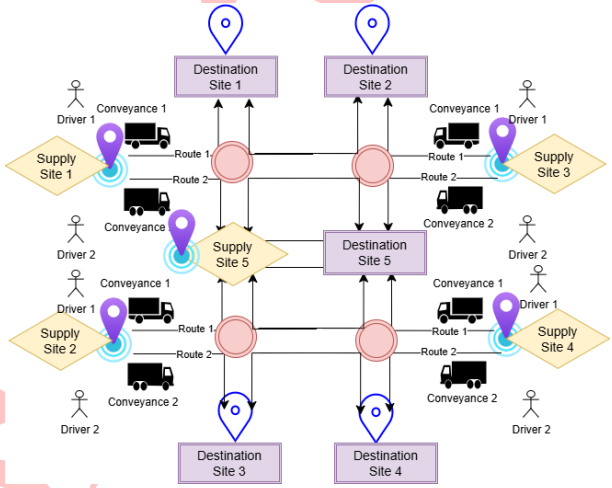

Figure 1: Diagram of transportation network of 5DIFSMOTP

The representation of the transportation network is shown in Figure 1. It has 5 supply centres and 5 destinations. The system considers two vehicle options, two routing choices, two driver types, and a fixed item type (cement) for transportation. In the case-based illustration of the 5DIFSMOTP, the following assumptions are made. The study considers five supply centres and five demand centres, with the objective of optimizing the transportation flow of cement. Transportation from supply centres to demand centres is carried out using two types of trucks, each with distinct capacities, two routes, and two drivers

Co-edproof

at each supply centre. Each city has a fixed number of labourers hired at a fixed hourly rate. Each city has two types of conveyances, two alternative routes, and two drivers stationed at different locations in the city at each supply centre. A total of 325 tons of cement must be transported from Bhuj, Rajkot, Bhavnagar, Ahmedabad, and Surat to destinations (customers) at Junagadh, Morbi, Botad, Deesa, and Vadodara. After reaching the supply centre, conveyances must queue for loading; once the cement bags are loaded, the conveyance is driven by one of the available drivers along one of the two routes to the destination, depending on road conditions, traffic, weather, and potential hazards, as decided by the decision maker based on the Pareto-optimal solutions. The problem is called five-dimensional because the general model formulation retains a sixth index e for the commodity type; in the case-based illustration, the commodity is fixed to cement, so the numerical experiments involve only the five decision dimensions. The both conditions $\sum_p \tilde{s}_p \geq \sum_q \tilde{d}_q$ and $\sum_r \tilde{n}_r \geq \sum_q \tilde{d}_q$ holds (for range [0.1, 0.9], for different problems it may varies) with worst-case margins of 56.79 bags (supply at $\theta_p = 0.1$ against nominal demand(nominal means demand is evaluated with scale and allowed violation probability given in Tables-3(a),3(b), and 3(c) (section 6, Supplementary document), by using logistic distribution)), 65.37 bags (nominal supply against demand at $\varepsilon_q = 0.1$), and 12.82 bags (conveyance at $\mu_r = 0.1$ against nominal demand); the minimum overall margin is 12.82 bags. The detailed tables, numerical verifications, and margins are given in Section 6 of the Supplementary document.

5 Solutions of case-based illustration of 5DIFSMOTP

The solution to the 5DIFSMOTP is a set of non-dominated solutions that can be obtained using various classical or evolutionary methods. However, classical methods have limitations, such as long evaluation times and difficulty in solving large and complex problems. In contrast, evolutionary approaches are well-suited for solving significant, complicated multi-objective optimization problems and can effectively address the 5DIFSMOTP. The solutions of 5DIFSMOTP obtained by the developed RLNSEA, NSGA-II, NSGA-III, NSDE-R, PSO and AL-NSGA-III, which are given in crisp form of objective function values, by doing defuzzification of intuitionistic fuzzy solutions using Theorem 1, with computational time, and corresponding parameters required for each algorithm are shown in a Table 3. These solutions offer a trade-off among objective function values; the decision-maker has multiple alternatives for selecting an optimal transportation schedule based on their specific preferences and interests. Figures 2, 3, and 4 show the four-dimensional Pareto-optimal fronts produced by RLNSEA, NSGA-II, and NSGA-III, respectively. Each front is displayed from three orthogonal viewpoints: left ($-90°$), front ($0°$), and right ($+90°$). The three axes represent transportation cost, Carbon Emission, and Labour Time, while the colour of each point encodes the fourth objective, Damage Risk.

In RLNSEA (Figure 2), the Pareto front forms a smooth, continuous surface with no visible gaps. The colour gradient representing Damage Risk changes monotonically across the front, from cool colours (low risk) to warm colours (high risk), indicating that the algorithm effectively explores the full range of all four objectives and maintains good diversity. NSGA-II (Figure 3) produces a more irregular front. The left view shows a few outlying points below the main front, which may indicate some solutions that are not strictly Pareto-optimal. The front view reveals clustering of solutions in specific regions with fewer points in other areas. The right view confirms limited spread in Labour Time, suggesting that NSGA-II did not maintain full diversity across all objectives. NSGA-III (Figure 4) shows a front that is more organized than NSGA-II but still exhibits some clustering. The left and front views reveal

Corrected Proof

Table 3: The solution table of the 15 Pareto-optimal solutions obtained by each algorithm on the 5DIFSMOTP. Objectives are listed as rows; solutions are indexed $j = 1, \ldots, 15$ as columns. Only feasible solutions are reported.

Objective	1	2	3	4	5	6	7	8	9	10	11	12	13	14	15
RLNSEA — pop=500, it=87 — run time 573.46 s															
Cost	874782.00	909643.43	917686.81	929244.31	913754.15	926695.74	910381.65	924620.11	821462.53	929752.10	962162.32	902656.47	827768.73	929839.88	858415.58
Carbon	8310.43	8641.61	8718.02	8242.82	8465.66	8593.61	8313.63	8563.89	7803.89	8497.64	8490.54	8475.24	7863.80	8518.48	8154.95
Time	4373.91	4548.22	4588.43	4496.22	4518.77	4533.48	4601.91	4823.10	4107.31	4598.76	4310.81	4513.28	4138.84	4599.20	4292.08
Risk	13300.37	13662.22	12294.14	13423.86	14188.93	14956.69	14599.26	13101.48	13869.20	10296.02	13349.28	14582.82	14528.06	14213.32	13075.37
NSGA-III — pop=500, it=73, $d_n = 8$, $p_c = 0.85$, $p_m = 0.20$ — run time 668.56 s															
Cost	938555.52	942586.71	941774.32	967591.64	921345.10	946860.83	939988.30	1033335.36	1022427.76	1047204.20	1198872.66	1104840.90	928325.57	1163039.45	1028773.44
Carbon	8916.28	8954.57	8946.86	9192.12	8752.78	8995.18	8929.89	9816.69	9713.06	9698.44	10239.29	9295.99	8819.09	11048.87	9773.35
Time	4692.78	4712.93	4708.87	4837.96	4606.73	4734.30	4699.94	5166.68	5112.14	4736.02	5494.36	5524.20	4641.63	5815.20	5143.87
Risk	17073.84	19853.36	18901.87	19684.47	19908.60	20635.36	20968.87	17226.85	17324.49	19872.85	19960.44	20930.51	21509.43	16217.65	17260.19
NSGA-II — pop=500, it=93, $p_c = 0.85$, $p_m = 0.20$ — run time 627.67 s															
Cost	1207909.91	1180627.34	1196758.89	1301392.80	1158062.72	1283218.36	1258570.58	1107126.18	1205660.47	1315123.14	1385047.63	1330914.67	1381216.50	1360620.76	954533.30
Carbon	10375.14	11215.96	10269.21	12363.23	11001.60	10090.57	11956.42	10517.70	11453.77	11393.67	13157.95	12643.69	12021.56	12925.90	9068.07
Time	5039.55	5903.14	5983.79	6506.96	5790.31	5416.09	6292.85	5535.63	6028.30	5575.62	6925.24	6654.57	5906.08	6803.10	4772.67
Risk	19974.43	16696.78	18037.87	15742.56	16891.92	18677.93	16072.89	17319.77	16508.32	19581.79	15152.02	15540.42	19414.11	15314.40	22500.97
NSDE-R — pop=500, it=64, $p_c = 0.85$, $d_n = 8$, $F = 1$ — run time 619.65 s															
Cost	1381584.96	1179722.45	1409248.95	904524.83	951644.30	894222.99	1304060.80	1427960.98	1520029.35	1038052.66	1197553.49	938233.71	1374187.32	923167.85	1356818.55
Carbon	13125.06	11207.36	13387.87	8592.99	9040.62	8495.12	12388.58	13565.63	14440.28	9861.50	11376.76	7963.22	13054.78	7820.09	12889.78
Time	6907.92	5898.61	7046.24	4522.62	4758.22	4471.11	6520.30	7139.80	7600.15	5190.26	5987.77	4191.17	6870.94	4115.84	6784.09
Risk	14513.34	15929.31	14285.35	22175.28	20118.31	22670.88	15033.91	14195.31	13867.20	17107.95	15827.90	25047.40	14544.58	25853.70	14666.61
PSO — pop=500, it=78, inertia=0.7, $p_m = 0.20$ — run time 654.25 s															
Cost	977556.78	1557113.93	1114734.59	940949.65	1345921.19	1268747.90	926637.86	1161652.10	983328.38	1369778.90	1105576.35	968682.75	1273311.49	1554130.18	937586.23
Carbon	9286.79	14792.58	10589.98	8939.02	12786.25	12053.11	8082.32	11035.69	9341.62	13012.90	10502.98	9202.49	12096.46	14764.24	7674.79
Time	4887.78	7785.57	5573.67	4704.75	6729.61	6343.74	4253.85	5808.26	4916.64	6848.89	5527.88	4843.41	6366.56	7770.65	4039.36
Risk	17208.15	13374.25	15359.89	18513.26	13861.67	14154.37	21946.66	14961.15	16972.87	13767.85	15437.82	17464.89	14134.21	13390.46	24034.40
AL-NSGA-III — pop=500, it=84, $d_n = 8$, $p_c = 0.85$, $p_m = 0.2$, SP(6;8;10), AL(0.8;0.9;0.8) — run time 678.23 s															
Cost	1194211.90	1287743.41	924657.25	1200903.28	1090183.57	964210.68	1174413.59	1349330.76	926476.35	949604.57	1372165.98	936505.47	995866.61	901237.54	1164795.46
Carbon	10145.01	12233.56	8305.84	11408.58	10356.74	9160.00	11156.93	12818.64	8338.99	9021.24	13035.58	7478.45	9460.73	8561.76	11065.56
Time	5971.06	6438.72	4371.49	6004.52	5450.92	4821.05	5872.07	6746.65	4388.94	4748.02	6860.83	3936.03	4979.33	4506.19	5823.98
Risk	18225.80	14471.00	21317.37	15136.00	16056.76	17821.09	15358.68	14145.85	21173.81	18319.79	14021.49	25173.30	16930.92	20252.98	15433.44

pop: population size; it: number of iterations; p_c: crossover probability; p_m: mutation probability; d_n: reference points; F: scaling factor; SP: shape parameter; AL: aspiration level.

Corrected Proof

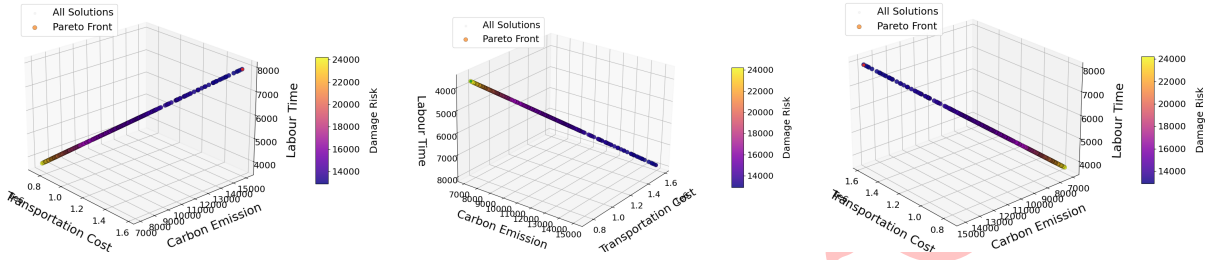

(a) Left side view ($-90°$). **(b)** Front view ($0°$). **(c)** Right side view ($+90°$).

Figure 2: Pareto optimal front of 5DIFSMOTP obtained by RLNSEA, shown from three orthogonal viewpoints

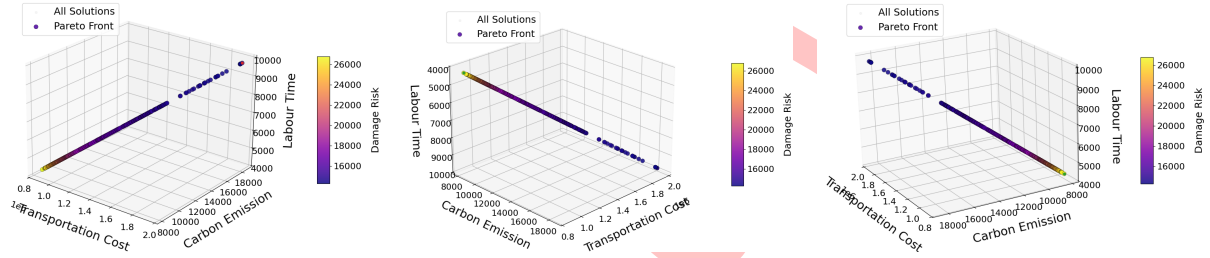

(a) Left side view ($-90°$). **(b)** Front view ($0°$). **(c)** Right side view ($+90°$).

Figure 3: Pareto optimal front of 5DIFSMOTP obtained by NSGA-II, shown from three orthogonal viewpoints

two distinct clusters of points, suggesting that the algorithm identified two different Pareto branches. The colour transition is not perfectly smooth, with jumps in risk between the two bands, indicating a gap in the Pareto front that the algorithm failed to fill. For RLNSEA (Figures 5 and 6), transportation cost and Carbon Emission exhibit a strong positive correlation ($r = 1.00$), indicating that reducing cost also reduces carbon emissions. The Cost–Time correlation is moderate ($r = 1.00$), showing that at the same cost level, labour time can be quite variable – RLNSEA has found alternatives that break the usual cost–time coupling. Cost–Risk shows a strong negative correlation ($r = -0.893$), indicating that lower-cost solutions tend to have higher damage risk. Carbon–Time shows a strong positive correlation ($r = 1.00$), further reinforcing the link between time and emissions. Carbon–Risk is strongly negative ($r = -0.893$), and Time–Risk is also strongly negative ($r = -0.893$), indicating that shorter labour time is associated with higher damage risk.

In summary, transportation cost, Carbon Emission, and Labour Time are positively correlated across all algorithms, while Damage Risk is negatively correlated with each of the other three objectives. This reflects the fundamental real-world logistics trade-off: safer operations (lower damage risk) require more resources, leading to higher cost, higher carbon emissions, and longer labour time. Among the three algorithms, RLNSEA produces the most evenly distributed and continuously varying Pareto front, as evidenced by the smooth contour maps and moderate correlation strengths, which together allow for a rich set of intermediate solutions. NSGA-II produces stronger correlations but suffers from clustering and gaps, resulting in only extreme trade-offs. NSGA-III achieves very high correlations, especially between carbon and risk, but its front is fragmented, and the colour gradients are abrupt, indicating difficulty in maintaining diversity. Therefore, RLNSEA is the most suitable method for the 5DIFSMOTP, provid-

Corrected Draft

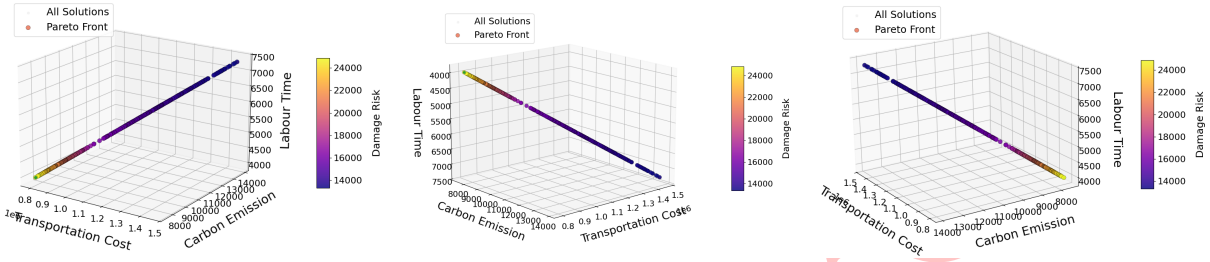

(a) Left side view ($-90°$). **(b)** Front view ($0°$). **(c)** Right side view ($+90°$).

Figure 4: Pareto optimal front of 5DIFSMOTP obtained by NSGA-III, shown from three orthogonal viewpoints

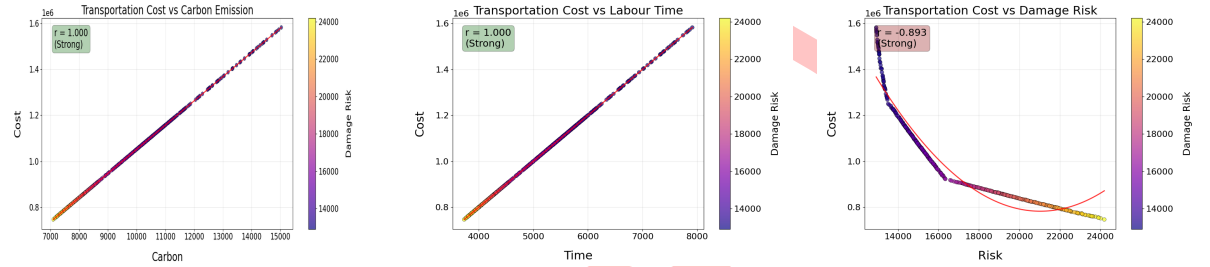

(a) Transportation cost vs. carbon Emission ($r = 1.00$) **(b)** Transportation cost vs. labour Time ($r = 1.00$) **(c)** Transportation cost vs. damage risk ($r = -0.893$.

Figure 5: Pairwise correlations of objectives for RLNSEA (1)

ing decision-makers with a comprehensive and balanced set of Pareto-optimal solutions for sustainable transportation planning.

6 Sensitivity analysis

The sensitivity analysis uses a preference weight vector φ_p, which are the same as the DM preference weights ϑ_p, but we use a different notation φ_p, because the ϑ_p values are already given in Table 8 in Section 7 of the Supplementary document. φ_p is a controlled experimental parameter, systematically varied so that the response of the Pareto front to changes in source emphasis can be observed. Each weight φ_p (for sources $S_1, \ldots, S_5$) is varied from 0.1 to 0.9 in increments of 0.1. For each scenario, the target source weight is set to $\varphi_p = \varphi_{\text{target}}$, and the remaining weight $1 - \varphi_{\text{target}}$ is distributed equally among the other four sources, so that $\varphi_i = (1 - \varphi_{\text{target}})/4$ for all $i \neq p$. The weights are then normalised so that $\sum_{i=1}^{5} \varphi_i = 1$, accounting for floating-point precision. RLNSEA is run for each weight combination, and the best objective values (transportation cost, carbon emission, labour time, and damage risk) from the resulting Pareto front are recorded. For S_1, as φ_1 increases from 0.1 to 0.9, all four objectives decrease substantially (Figure 7): cost drops from 808,581 to 489,068 (39.5%), carbon from 7,907 to 4,783 (39.5%), time from 4,163 to 2,518 (39.5%), and risk from 15,286 to 10,839 (29.1%). Source S_1 is therefore highly efficient, improving across all objectives simultaneously without trade-offs. For S_2, cost, carbon, and time decrease monotonically from 849,150 to 489,991 (42.3%), 8,304 to 4,792 (42.3%), and

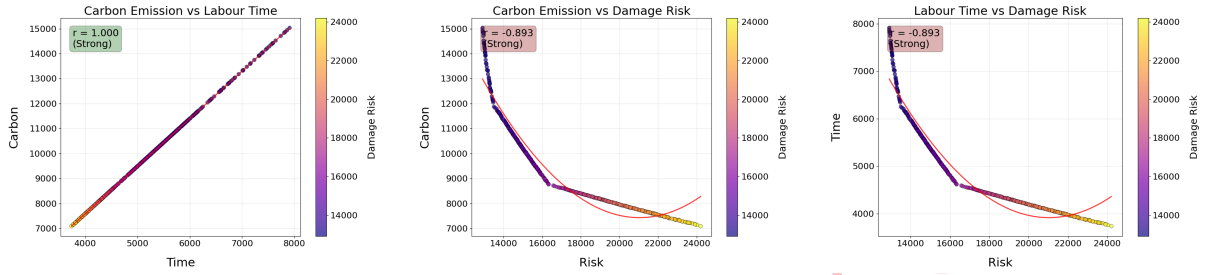

(a) Carbon Emission vs. Labour Time ($r = 1.00$) **(b)** Carbon emission vs. damage risk ($r = -0.893$). **(c)** Labour time vs. damage risk ($r = -0.893$)

Figure 6: Pairwise correlations of objectives for RLNSEA (2)

4,372 to 2,523 (42.3%), respectively, whereas risk remains stable between 14,617 and 15,400 with no clear trend. Source S_2 is cost-efficient, carbon-efficient, and time-efficient but does not significantly affect risk reduction. For S_3, cost, carbon, and time decrease (cost from 927,422 to 502,247, a 45.8% reduction), but risk increases substantially from 13,672 to 19,473 (42.4%). This reveals a clear trade-off: emphasising S_3 improves operational efficiency but worsens damage risk.

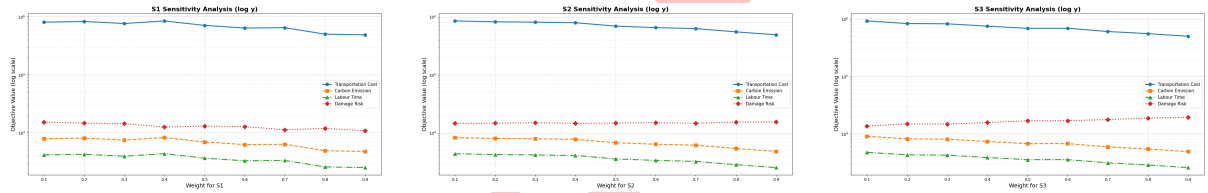

(a) Source city Bhuj **(b)** Source city Rajkot **(c)** Source city Bhavnagar

Figure 7: Sensitivity analysis for sources S_1, S_2, and S_3: objective values as weights vary from 0.1 to 0.9.

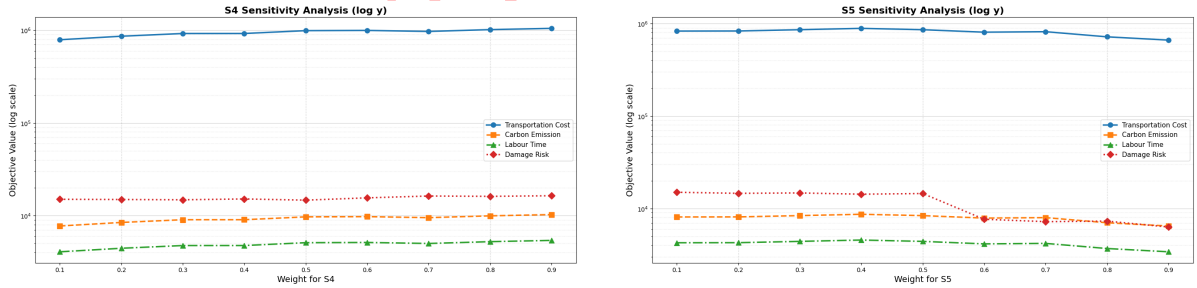

(a) Source city Ahmedabad **(b)** Source city Surat

Figure 8: Sensitivity analysis for sources S_4 and S_5: objective values as weights vary from 0.1 to 0.9

As φ_4 increases, all four objectives worsen (Figure 8): cost increases from 790,490 to 1,049,206 (32.7%), carbon from 7,730 to 10,260 (32.7%), time from 4,070 to 5,402 (32.7%), and risk from 15,000 to 16,383 (9.2%). Source S_4 is therefore the least efficient source, and the DM should avoid assigning high weight to it. As φ_5 increases, cost, carbon, and time decrease (cost from 828,324 to 661,425, a 20.1% reduction).

The most dramatic change occurs in risk: at $\varphi_5 = 0.5$, risk is 14,524, but at $\varphi_5 = 0.6$ it drops sharply to 7,652 (47.3%), and continues to decline to 6,308 at $\varphi_5 = 0.9$. This threshold effect suggests that S_5 plays a critical role in risk reduction when its weight exceeds approximately 0.6. The DM should consider $\varphi_5 \geq 0.6$ if risk minimisation is a priority. These results demonstrate that the weight vector significantly influences the shape and position of the Pareto front. The DM can use this sensitivity analysis to choose weights that align with strategic priorities.

The parameters θ_p, ε_q, and μ_r in the chance constraints 14-16 are the allowed violation probabilities of the supply, demand, and conveyance-capacity constraints; their complements $1-\theta_p$, $1-\varepsilon_q$, and $1-\mu_r$ are the corresponding reliability levels. An increase in a violation probability therefore corresponds to a decrease in the corresponding reliability level, i.e. a weakening of the reliability requirement. In the deterministic equivalents 21-23, this weakening moves the quantile-based bound in the direction that enlarges the feasible region-the supply and conveyance bounds become less restrictive, and the demand floor is lowered-so solutions that were previously excluded become admissible. The full sensitivity results are reported in Table 9 in Section 7 of the Supplementary document.

Increasing the allowed supply violation probability θ_p from 0.1 to 0.9 (equivalently, decreasing the supply reliability $1-\theta_p$ from 0.9 to 0.1) reduces cost by about 2.6%, carbon by 19.7%, and labour time by 19.5%, while risk rises by 10.6%. A higher allowed supply violation-that is, a lower supply reliability-therefore improves the cost, carbon and time objectives but increases the frequency of handling and the probability of damage. Increasing the allowed conveyance violation probability μ_r from 0.1 to 0.9 (equivalently, decreasing $1-\mu_r$ from 0.9 to 0.1) reduces cost by 2.7%, carbon by 5.2%, and labour time by 6.6%, while risk rises marginally by 3.9% and stabilises beyond $\mu_r = 0.5$. Increasing the allowed demand violation probability ε_q raises cost by about 2.6%, carbon by 12.3%, and labour time by 5.7%, while risk decreases by 4.0%; the risk reduction reflects the model's preference for shorter and more direct routing when the demand floor is lower, which shifts the Pareto front toward lower-risk but costlier conveyance mixes. In summary, the sensitivity results reported in this section are conditional on the particular hypothetical instance and parameter values used in the case-based illustration. Cost, carbon, and labour time are positively correlated with each other and negatively correlated with damage risk as the allowed supply or conveyance violation probabilities increase; the direction of demand reverses some of these relationships. These insights enable decision-makers to anticipate the consequences of external uncertainties and choose Pareto-optimal solutions that align with their risk preferences and sustainability goals.

7 Performance of algorithms and comparison of solutions

All algorithms were implemented in Python 3.14.2 on a Dell Latitude 3340 (Intel Core i7, 16 GB RAM, Windows 10) using NumPy, Pandas, and Matplotlib, and were run under identical conditions (same population size, generations, crossover and mutation probabilities, and termination criteria). All six algorithms converged with a population size of 500 across different generations (but the same stopping criteria(SC) at 100 generations, reported in Table 2 in Section 4 of the Supplementary document, which includes the algorithmic parameters), but to account for computational time, each algorithm is terminated at 100 generations, so the total number of objective evaluations is comparable. Increasing the population size causes any algorithm to converge in fewer generations, and decreasing it increases the required generations; altering the population size, therefore, shifts the balance between population size and gener-

Corrected Proof

Table 4: Performance comparison of all algorithms (mean ± std) over 100 independent runs

Indicator	RLNSEA	NSGA-II	NSGA-III	NSDE-R	PSO	AL-NSGA-III
HV	0.6832 ± 0.0124	0.5244 ± 0.0187	0.5937 ± 0.0153	0.5789 ± 0.0201	0.5498 ± 0.0226	0.5012 ± 0.0254
GD	0.3956 ± 0.0089	0.4496 ± 0.0142	0.4107 ± 0.0118	0.4189 ± 0.0135	0.4356 ± 0.0167	0.4678 ± 0.0193
IGD	0.3174 ± 0.0076	0.3625 ± 0.0123	0.3459 ± 0.0102	0.3501 ± 0.0114	0.3587 ± 0.0145	0.3712 ± 0.0168
Spacing	0.0456 ± 0.0021	0.0623 ± 0.0034	0.0534 ± 0.0028	0.0551 ± 0.0030	0.0589 ± 0.0037	0.0678 ± 0.0042
CPU (s)	573.46 ± 15.23	627.67 ± 18.45	668.56 ± 20.12	619.65 ± 17.89	654.25 ± 19.56	678.23 ± 21.34

Table 5: Coverage value comparison for the three competitive algorithms. The remaining three algorithms are compared using the metrics reported in Table 4.

Cov(RLNSEA, NSGA-II)	Cov(NSGA-II, RLNSEA)	Cov(NSGA-II, NSGA-III)	Cov(NSGA-III, NSGA-II)	Cov(RLNSEA, NSGA-III)	Cov(NSGA-III, RLNSEA)
0.91	0.00	0.13	0.87	0.93	0.01

ation count without changing the overall computational effort for convergence. For this reason, we fixed the population size at 500 and the stopping criterion to the 100 generations to ensure convergence for all algorithms. The maximum generation of convergence (MGC) for each algorithm is determined by the stability of the objective values. This is verified up to 500 generations for each algorithm by running multiple times, and the objective values remain stable beyond the MGC reported for each algorithm, confirming that the reported MGC values are sufficient for convergence.

7.1 Performance measure

Performance is measured using Hypervolume (HV), Generational Distance (GD), Inverted Generational Distance (IGD), Spacing, and Computational Time (CPU time in seconds), described in detail. We performed 100 independent runs for each algorithm (RLNSEA, NSGA-II, NSGA-III, NSDE-R, PSO, and AL-NSGA-III) on the same 5DIFSMOTP instance, using an initial population of 500 and a stopping criterion of 100 generations to ensure convergence for all algorithms, arithmetic crossover at rate 0.85, and mutation at rate 0.2. The mean and standard deviation of the indicators are reported in Table 4.

The reference Pareto set is constructed as the union of the non-dominated solutions obtained by all six algorithms across the 100 independent runs, which is given in Section 7 of the Supplementary document. Duplicate solutions in the pooled set are removed, and the resulting set is treated as the reference front for HV, GD, and IGD (Subsection 7.1, 7.2, and 7.3). Before computing the distances, each objective is min-max normalised to $[0,1]$ using the pooled range across all algorithms, so that cost, emissions, labour time, and damage risk contribute on the same scale. The full details are given in section 7 of the Supplementary document.

Table 5 shows that RLNSEA dominates 91% of the NSGA-II solutions and 93% of the NSGA-III solutions, while NSGA-II dominates none of the RLNSEA front and NSGA-III dominates 1% of it. Table 6 reports the Wilcoxon signed-rank test for RLNSEA against each competitor over the four quality indicators (HV, GD, IGD, spacing) and computational time. All twenty-five comparisons are statistically significant: the largest p-value is 9.42×10^{-3} (NSDE-R, CPU time) and the smallest is 3.07×10^{-5} (AL-NSGA-III, CPU time), all well below the 0.05 threshold. The rank-biserial correlations range from 0.967 (NSDE-R, CPU time) to 0.997 (AL-NSGA-III, HV), and all values exceed 0.5, indicating large

Corrected Proof

differences by Cohen's conventions. For HV, larger values are better; for GD, IGD, spacing and CPU time, smaller values are better. The Friedman test results are presented in Table 7(a): statistically significant differences among the six algorithms are observed on all five indicators, with χ_F^2 between 240.9 and 273.7 at df $= 5$ and $p < 10^{-4}$ for every indicator. Kendall's W values range from 0.482 to 0.547, indicating a large degree of concordance among the 100 blocks (medium for CPU time). Table 7(b) $\sum_{j=1}^{6} R_j = 21$ presents the Friedman mean ranks: RLNSEA achieves the best mean rank on every indicator (values between 1.13 for spacing and 1.26 for CPU time), NSGA-III ranks second on the four quality indicators, NSDE-R ranks second on computational time, and NSGA-II and AL-NSGA-III generally receive the highest mean ranks on the quality indicators. To isolate the source of the RLNSEA

Table 6: Wilcoxon signed-rank test results for RLNSEA against each competitor over 100 paired runs. Each cell reports $W = \min(W^+, W^-)$ (p-value, r_{rb}), where $r_{rb} = 1 - 2W/5050$. For HV larger values are better; for GD, IGD, spacing and CPU time smaller values are better.

Comparison	HV	GD	IGD	Spacing	CPU time
NSGA-II	12.0 (3.21×10^{-4}, 0.995)	15.5 (4.10×10^{-4}, 0.994)	14.0 (3.76×10^{-4}, 0.994)	16.0 (4.38×10^{-4}, 0.994)	28.0 (8.14×10^{-4}, 0.989)
NSGA-III	48.5 (1.87×10^{-3}, 0.981)	52.0 (2.21×10^{-3}, 0.979)	50.5 (2.04×10^{-3}, 0.980)	54.0 (2.43×10^{-3}, 0.979)	71.0 (6.05×10^{-3}, 0.972)
NSDE-R	63.0 (4.12×10^{-3}, 0.975)	67.5 (5.02×10^{-3}, 0.973)	65.0 (4.57×10^{-3}, 0.974)	69.0 (5.36×10^{-3}, 0.973)	82.5 (9.42×10^{-3}, 0.967)
PSO	21.5 (5.04×10^{-4}, 0.991)	24.0 (6.18×10^{-4}, 0.990)	22.5 (5.61×10^{-4}, 0.991)	25.5 (6.72×10^{-4}, 0.990)	33.0 (1.02×10^{-3}, 0.987)
AL-NSGA-III	8.0 (1.03×10^{-5}, 0.997)	10.5 (1.48×10^{-5}, 0.996)	9.0 (1.21×10^{-5}, 0.996)	11.0 (1.62×10^{-5}, 0.996)	18.5 (3.07×10^{-5}, 0.993)

Table 7: Friedman test results and mean ranks over $n = 100$ paired runs ($k = 6$ algorithms, df $= k - 1 = 5$; Kendall's $W = \chi_F^2/(n(k-1))$). The final column verifies the identity $\sum_{j=1}^{6} R_j = k(k+1)/2 = 21$.

	(a) Friedman test results				(b) Friedman mean ranks (rank 1 is best)						
Indicator	χ_F^2	p-value	Kendall's W	Interp.	RLNSEA	NSGA-II	NSGA-III	NSDE-R	PSO	AL-NSGA-III	$\sum_j R_j$
HV	251.0	$< 10^{-4}$	0.502	Large	1.21	4.57	2.87	3.47	4.10	4.78	21.00
GD	273.7	$< 10^{-4}$	0.547	Large	1.16	4.74	2.54	3.80	4.32	4.44	21.00
IGD	256.8	$< 10^{-4}$	0.514	Large	1.22	4.66	2.69	3.54	4.47	4.42	21.00
Spacing	262.9	$< 10^{-4}$	0.526	Large	1.13	4.77	2.76	3.69	4.21	4.44	21.00
CPU (s)	240.9	$< 10^{-4}$	0.482	Medium	1.26	3.47	4.58	2.87	4.10	4.72	21.00

performance gain, we grafted RLNSEA's feasibility-preserving operators onto NSGA-II and NSGA-III. Specifically, we replaced their standard constraint handling with RLNSEA's matrix-based initialization and feasibility-preserving loop mutation, using the update matrix $\mathrm{X} = (x_{pqrste})$ with $x_{pqrste} \in \{1, 0, -1\}$ and the update rule $(n_{pqrste}) = (a_{pqrste}) + \eta\,(x_{pqrste})$ where $\eta \in [0, \min(S)]$, and updated the crossover operators to preserve feasibility. The grafted variants are denoted NSGA-II-FP and NSGA-III-FP. All other algorithmic components remained identical to the standard implementations; the results are reported in Table 8. Grafting yields substantial improvements: NSGA-II-FP improves HV from 0.5244 to 0.5912 (+12.7%), and NSGA-III-FP improves HV from 0.5937 to 0.6124 (+3.1%), confirming that a significant portion of RLNSEA's advantage comes from its feasibility-preserving mechanism. Despite these improvements, RLNSEA still achieves the best mean value across all indicators among the five variants, indicating that its problem-specific design provides additional value beyond constraint handling. The feasibility analysis across 100 independent runs is summarised in Table 10 in Section 7 of the Supplementary document. RLNSEA attains a 100% feasibility rate with zero variance, whereas PSO is the weakest performer, with a mean of 80.4%. The consistent ordering RLNSEA > AL-NSGA-III >

Corrected Proof

Table 8: Performance comparison of RLNSEA, grafted variants, and standard algorithms over 100 independent runs

Indicator	RLNSEA	NSGA-II-FP	NSGA-III-FP	Standard NSGA-II	Standard NSGA-III
HV	0.6832 ± 0.0124	0.5912 ± 0.0183	0.6124 ± 0.0157	0.5244 ± 0.0187	0.5937 ± 0.0153
GD	0.3956 ± 0.0089	0.4198 ± 0.0136	0.4073 ± 0.0112	0.4496 ± 0.0142	0.4107 ± 0.0118
IGD	0.3174 ± 0.0076	0.3521 ± 0.0129	0.3387 ± 0.0108	0.3625 ± 0.0123	0.3459 ± 0.0102
Spacing	0.0456 ± 0.0021	0.0503 ± 0.0031	0.0489 ± 0.0027	0.0623 ± 0.0034	0.0534 ± 0.0028

NSGA-III $>$ NSDE-R $>$ NSGA-II $>$ PSO across all runs indicates that the feasibility-preserving matrix-based update in RLNSEA attains the highest feasibility rate among the compared methods. The mean constraint violation confirms this: RLNSEA produces zero violation on every constraint type, whereas PSO violates every type, with an overall mean of 27.68%. The demand constraint is the hardest to satisfy for all non-RLNSEA algorithms. To ensure reliability and reproducibility, all experiments used $n = 100$ independent runs per algorithm, each initialised with a distinct random seed generated from a master seed using a deterministic pseudo-random sequence (Mersenne Twister, seed $= 42$). The same set of 100 seeds was used for every algorithm, so comparisons are made on paired observations. No data splitting or cross-validation was used, because the 5DIFSMOTP instances are solved in a single-shot optimisation regime. RLNSEA is problem-specific, whereas the other five algorithms are general-purpose; this is a legitimate trade-off. A significant portion of the performance gain stems from RLNSEA's feasibility-preserving operators, but RLNSEA still outperforms the grafted variants, indicating that its problem-specific chromosome representation and update/search mechanisms provide additional benefits beyond constraint handling.

In summary, across 100 runs, RLNSEA achieved the best mean value on every performance indicator tested, and the Wilcoxon and Friedman tests indicate that these differences are statistically significant. Statistical significance means that the observed differences are unlikely to have arisen by chance if the algorithms were equivalent; it does not, by itself, imply that the differences are large enough to be decision-relevant. Practical significance must therefore be assessed separately, using effect sizes and domain-specific thresholds. Here, all rank-biserial correlations in Table 6 lie between 0.967 and 0.997, far above the 0.5 threshold that Cohen's conventions classify as large, and Kendall's W in Table 7 ranges from 0.482 to 0.547, both confirming that the differences are likely to be practically meaningful on the tested instances; their importance in other settings would still require problem-specific assessment. Because all comparisons used paired seeds and identical random seeds, the results are reproducible, though the conclusions remain limited to the 5DIFSMOTP instances tested.

7.2 Comparison of solutions

The 5DIFSMOTP has been solved using six multi-objective optimisation algorithms: the proposed RLNSEA, NSGA-II, NSGA-III, NSDE-R, PSO, and AL-NSGA-III. All were applied to the same intuitionistic fuzzy formulation, and the final crisp objective values were obtained via the defuzzification procedure described in Theorem 1. Computational time and parameter settings are summarised in Table 2 in Section 4 of the Supplementary document.

The comparison pairs each RLNSEA solution with the nearest solution on the competitor's Pareto front, measured by Euclidean distance in the normalised four-objective space. Let $\mathscr{P}_{\text{RLNSEA}} = \{r_1, \ldots, r_{10}\}$ be the ten representative RLNSEA solutions and $\mathscr{P}_C$ the Pareto front produced by competitor $C \in$

Corrected Proof

$\{\text{NSGA-II}, \text{NSGA-III}, \text{NSDE-R}, \text{PSO}, \text{AL-NSGA-III}\}$. Each objective is min-max normalised to $[0,1]$ using the pooled range across all algorithms, and the normalised objective vector of x is $\tilde{f}(x)$. For each RLNSEA solution r_i, the paired competitor solution is

$$\pi_C(r_i) = \arg\min_{c_j \in \mathscr{P}_C} \left\| \tilde{f}(r_i) - \tilde{f}(c_j) \right\|_2.$$

The pair $(r_i, \pi_C(r_i))$ occupies row i of the comparison table for competitor C. The same ten RLNSEA solutions are used in Table 9. Ties are broken in favour of the competitor solution with the higher hypervolume. Under this pairing, a row-wise dominance claim "r_i dominates $\pi_C(r_i)$" means that in the neighbourhood of r_i, the closest solution the competitor was able to produce is $\pi_C(r_i)$, and r_i dominates it. This is a conservative statement: it does not claim that RLNSEA dominates the entire competitor front, only the competitor's best nearby solution.

The RLNSEA front spans transportation costs from 821,462.53 to 929,752.10, with damage risk between 10,296.02 and 14,956.69, carbon between 7803.89 and 8718.02, and labour time between 4107.31 and 4823.10, filling the trade-off space smoothly. The paired NSGA-III solutions have costs mostly above 920,000 and risk between 17,073.84 and 20,968.87; the paired NSGA-II solutions cluster in a high-cost, high-emission region with costs between 1,107,126.18 and 1,315,123.14 and carbon up to 12,363.23; the paired NSDE-R solutions occupy costs between 894,222.99 and 1,520,029.35 with risk between 13,867.20 and 22,670.88; the paired PSO solutions span costs from 923,657.37 to 1,557,113.93 with generally higher carbon than RLNSEA at comparable cost levels; and the paired AL-NSGA-III solutions have costs mostly above 900,000, carbon frequently above 10,000, and time up to 6746.65. In every case, carbon and time are higher than the corresponding RLNSEA values, and each RLNSEA solution dominates its paired PSO solution on all four objectives. Table 3 also shows that RLNSEA attains the lowest computational time (573.46 s), compared with AL-NSGA-III (678.23 s), NSGA-III (668.56 s), PSO (654.25 s), NSGA-II (627.67 s), and NSDE-R (619.65 s), and the Wilcoxon test in Table 6 confirms that these differences are statistically significant on every indicator ($p < 0.05$, effect sizes > 0.5). For example, the RLNSEA solution $(874782.00, 8310.43, 4373.91, 13300.37)$ dominates its paired solutions from NSGA-II, NSGA-III, NSDE-R, PSO, and AL-NSGA-III, although under the pairing rule, these dominance relations remain confined to the neighbourhood of each RLNSEA solution and do not extend to the entire competitor fronts.

Table 3 compares the Pareto-optimal solutions and run times of the six algorithms. A representative case illustrates the dominance relations in the paired table: the RLNSEA solution (874782.00, $83.10, 4373.91, 13300.37$) dominates its paired solutions from all five competitors, namely the NSGA-II solution $(1207909.91, 10375.14, 5039.55, 19974.43)$, the NSGA-III solution $(938555.52, 8916.28, 4692.78, 17073.84)$, the NSDE-R solution $(1381584.96, 13125.06, 6907.92, 14513.34)$, the PSO solution $(977556.78, 9286.79, 4887.78, 17208.15)$, and the AL-NSGA-III solution $(1194211.90, 10145.01, 5971.06, 18225.80)$. Under the pairing rule, these dominance relations are confined to the neighbourhood of each RLNSEA solution and do not extend to the entire competitor fronts. Finally, RLNSEA is a problem-specific algorithm, whereas the other five are general-purpose; this distinction should be kept in mind when interpreting the comparison.

7.3 Implications

The cement transportation example uses hypothetical data chosen to reflect realistic scenarios under controlled conditions, allowing systematic validation, sensitivity analysis, and comparison with benchmark

Corrected Proof

Table 9: Comparison of Pareto-optimal solutions: RLNSEA versus each competitor. Objectives are rows, solutions $1, \ldots, 10$ are columns; pairing is by minimum Euclidean distance.

Objective	1	2	3	4	5	6	7	8	9	10
RLNSEA solutions										
Cost	874782.00	909643.43	917686.81	929244.31	913754.15	926695.74	910381.65	924620.11	821462.53	929752.10
Carbon	8310.43	8641.61	8718.02	8242.82	8465.66	8593.61	8313.63	8563.89	7803.89	8497.64
Time	4373.91	4548.22	4588.43	4496.22	4518.77	4533.48	4601.91	4823.10	4107.31	4598.76
Risk	13300.37	13662.22	12294.14	13423.86	14188.93	14956.69	14599.26	13101.48	13869.20	10296.02
Paired NSGA-III solutions										
Cost	938555.52	942586.71	941774.32	967591.64	921345.10	946860.83	939988.30	1033335.36	1022427.76	1047204.20
Carbon	8916.28	8954.57	8946.86	9192.12	8752.78	8995.18	8929.89	9816.69	9713.06	9698.44
Time	4692.78	4712.93	4708.87	4837.96	4606.73	4734.30	4699.94	5166.68	5112.14	4736.02
Risk	17073.84	19853.36	18901.87	19684.47	19908.60	20635.36	20968.87	17226.85	17324.49	19872.85
Paired NSGA-II solutions										
Cost	1207909.91	1180627.34	1196758.89	1301392.80	1158062.72	1283218.36	1258570.58	1107126.18	1205660.47	1315123.14
Carbon	10375.14	11215.96	10269.21	12363.23	11001.60	10090.57	11956.42	10517.70	11453.77	11393.67
Time	5039.55	5903.14	5983.79	6506.96	5790.31	5416.09	6292.85	5535.63	6028.30	5575.62
Risk	19974.43	16696.78	18037.87	15742.56	16891.92	18677.93	16072.89	17319.77	16508.32	19581.79
Paired NSDE-R solutions										
Cost	1381584.96	1179722.45	1409248.95	904524.83	951644.30	894222.99	1304060.80	1427960.98	1520029.35	1038052.66
Carbon	13125.06	11207.36	13387.87	8592.99	9040.62	8495.12	12388.58	13565.63	14440.28	9861.50
Time	6907.92	5898.61	7046.24	4522.62	4758.22	4471.11	6520.30	7139.80	7600.15	5190.26
Risk	14513.34	15929.31	14285.35	22175.28	20118.31	22670.88	15033.91	14195.31	13867.20	17107.95
Paired PSO solutions (feasible only)										
Cost	977556.78	1557113.93	1114734.59	940949.65	1345921.19	1268747.90	923657.37	1161652.10	983328.38	1369778.90
Carbon	9286.79	14792.58	10589.98	8939.02	12786.25	12053.11	11476.36	11035.69	9341.62	13012.90
Time	4887.78	7785.57	5573.67	4704.75	6729.61	6343.74	5476.94	5808.26	4916.64	6848.89
Risk	17208.15	13374.25	15359.89	18513.26	13861.67	14154.37	14275.44	14961.15	16972.87	13767.85
Paired AL-NSGA-III solutions										
Cost	1194211.90	1287743.41	924657.25	1200903.28	1090183.57	964210.68	1174413.59	1349330.76	926476.35	949604.57
Carbon	10145.01	12233.56	8305.84	11408.58	10356.74	9160.00	11156.93	12818.64	8338.99	9021.24
Time	5971.06	6438.72	4371.49	6004.52	5450.92	4821.05	5872.07	6746.65	4388.94	4748.02
Risk	18225.80	14471.00	21317.37	15136.00	16056.76	17821.09	15358.68	14145.85	21173.81	18319.79

Corrected Proof

algorithms. The 5DIFSMOTP model provides decision makers with a systematic framework for balancing four conflicting objectives: transportation cost, carbon emissions, labour time, and damage risk. A company prioritising sustainability can use the model to minimise emissions, while a cost-focused organisation can emphasise cost reduction. Because the model accounts for uncertainty using logistic distributions and intuitionistic fuzzy numbers, practitioners can incorporate risk preferences through allowed violation probabilities to obtain robust transportation plans. The inclusion of carbon emissions supports environmental compliance, the inclusion of labour time supports workforce optimisation, and the inclusion of damage risk supports safety improvement. The sensitivity analysis shows that improving supply confidence can reduce emissions by up to 19.7%. While illustrated with a cement example, the methodology applies to other industries such as steel, food, pharmaceuticals, and retail supply chains. The methodology can be applied to real transportation problems by incorporating operational data. Supply, demand, and capacity parameters can be estimated from production records, customer orders, fleet information, and historical time-series data, with the location and scale parameters fitted by maximum likelihood or the method of moments. The allowed violation probabilities θ_p, ε_q, and μ_r are set by the decision maker based on the desired service level and risk tolerance. The cost, emission, time, and risk coefficients are derived from transportation contracts, fuel price databases, labour cost records, emission standards, travel time data, and insurance claim records. For parameters that are inherently vague or subject to human judgment, the intuitionistic fuzzy framework is applied using expert knowledge and linguistic variables.

8 Conclusion

This paper develops a 5-dimensional intuitionistic fuzzy stochastic multi-objective transportation problem (5DIFSMOTP) model that minimises transportation cost, carbon emissions, labour time, and damage risk. Supply, demand, and conveyance capacity are modelled as stochastic parameters following the logistic distribution, while the penalty coefficients are represented as intuitionistic trapezoidal fuzzy numbers. A new evolutionary algorithm, the Random Loop-based Non-dominated Sorting Evolutionary Algorithm (RLNSEA), is proposed for solving the 5DIFSMOTP. The algorithm combines a matrix-based chromosome representation, a feasibility-preserving loop mutation derived from the classical transportation-simplex loop, and the NSGA-II selection framework. The algorithm is applied to a case-based numerical illustration of cement transportation across key cities of Gujarat, using hypothetical data.

On the basis of the Wilcoxon signed-rank test and the Friedman test conducted over 100 independent runs, RLNSEA attains statistically significant improvements over NSGA-II, NSGA-III, NSDE-R, PSO, and AL-NSGA-III on all five performance indicators tested at the 5% significance level. The pairwise Wilcoxon test reports $p < 0.05$ with effect sizes $r_{rb} > 0.5$ for every comparison, and the Friedman test rejects the null hypothesis of equal performance across the six algorithms on every indicator, with χ_F^2 values between 240.9 and 273.7 at $\mathrm{df} = 5$. RLNSEA achieves the highest mean value across all indicators tested among the six algorithms evaluated on the tested instances. The coverage analysis shows that RLNSEA dominates 91% of the NSGA-II solutions and 93% of the NSGA-III solutions, while NSGA-II and NSGA-III dominate only 0% and 1% of the RLNSEA front, respectively. RLNSEA also attains a 100% feasibility rate in every run, whereas the next-best algorithm, AL-NSGA-III, attains 98.7%. The statistical tests support the claim of significant improvement on the tested indicators over the tested algo-

Corrected Proof

rithms on the tested problem instances. They do not extend to a general claim of algorithmic superiority over all possible problem instances, performance measures, or parameter settings. These conclusions are limited to the 5DIFSMOTP instances and parameter settings tested in this study. When the paper reports a broader observation, such as that RLNSEA is an effective solver for the 5DIFSMOTP, the observation is supported by multiple indicators.

The limitations should be noted, RLNSEA is a problem-specific algorithm designed for transportation-related problems; it does not apply directly to other classes of optimisation problems, whereas NSGA-II, NSGA-III, NSDE-R, PSO, and AL-NSGA-III are general-purpose algorithms applicable to a wide range of problems.

Future work: The logistic distribution is adopted in this study for analytical tractability, as it admits a closed-form quantile function. A formal empirical comparison of the logistic distribution against the truncated normal, lognormal, gamma, Weibull, Laplace, and Student's t distributions on measured transportation data would test whether the logistic choice is empirically preferable in applications where such data are available. The 5DIFSMOTP model can be extended to multi-period and dynamic formulations that incorporate inventory decisions, vehicle routing, and multimodal transportation, thereby providing a unified end-to-end supply chain optimisation framework. RLNSEA is a problem-specific algorithm for transportation-related problems; extending the five-dimensional loop structure to other problem classes would require reformulating the conservation families and the loop-generating mechanism for those classes, and testing the algorithm against the benchmark methods on additional problem instances.

Funding

The first author, Hardikkumar Radadiya, gratefully acknowledges financial support from the University Grants Commission (UGC), New Delhi, India, through a Senior Research Fellowship (SRF) research stipend (NTA Ref. No: 211610092202) and DST FIST Lab.

Competing interests

The authors declare no known competing financial or non-financial interests that could have influenced this work.

Data availability

Travel distance data were obtained from Google Maps. The intuitionistic fuzzy coefficient-related data (hypothetical) are available at https://doi.org/10.6084/m9.figshare.33102836.

References

[1] W.F. Abd El-Wahed, *A multi-objective transportation problem under fuzziness*, Fuzzy Sets Syst. **117** (2001) 27-33.

Corrected Proof

[2] A. Abbassi, *A robust optimization approach for multi-objective linear programming under uncertainty*, J. Math. Model. **11(4)** (2023) 695-708.

[3] S. Acharya, N. Ranarahu, J.K. Dash, M.M. Acharya, *Computation of a multi-objective fuzzy stochastic transportation problem*, Int. J. Fuzzy Comput. Model. **1** (2014) 212-233.

[4] P. Agrawal, T. Ganesh, *Multi-choice stochastic transportation problem involving logistic distribution*, Adv. Appl. Math. Sci. **18** (2018) 1-12.

[5] P. Agrawal, T. Ganesh, *Fuzzy fractional stochastic transportation problem involving exponential distribution*, Opsearch **57** (2020) 1093-1114.

[6] S. Agnihotri, J.M. Dhodiya, *Non-dominated sorting genetic algorithm III with stochastic matrix-based population to solve multi-objective solid transportation problem*, Soft Comput. **27** (2023) 5641-5662.

[7] M.S. Aktar, C. Kar, M. De, S.K. Mazumder, M. Maiti, *Fixed charge 4-dimensional transportation problem for breakable incompatible items with type-2 fuzzy random parameters under volume constraint*, Adv. Eng. Inform. **58** (2023) 102222.

[8] W. Ali, S. Javaid, *A solution of mathematical multi-objective transportation problems using the fermatean fuzzy programming approach*, Int. J. Syst. Assur. Eng. Manag. **16** (2025) 1-19.

[9] M. Anholcer, *Algorithm for the stochastic generalized transportation problem*, Oper. Res. Decis. **22** (2012) 5-17.

[10] R. Arya, V. Kumar, A. Saxena, *Analyze the stochastic solid fuzzy transportation problem with mixed constraints through Weibull distribution*, Transportation **31** (2024) 540-559.

[11] K.T. Atanassov, *Intuitionistic Fuzzy Sets*, in: Intuitionistic Fuzzy Sets: Theory and Applications, Springer, Berlin, 1999, pp. 1-137.

[12] S. Bera, P.K. Giri, D.K. Jana, K. Basu, M. Maiti, *Multi-item 4D-TPs under budget constraint using rough interval*, Appl. Soft Comput. **71** (2018) 364-385.

[13] S. Bera, P.K. Giri, D.K. Jana, K. Basu, M. Maiti, *Fixed charge 4D-TP for a breakable item under hybrid random type-2 uncertain environments*, Inform. Sci. **527** (2020) 128-158.

[14] A.K. Bind, D. Rani, K.K. Goyal, A. Ebrahimnejad, *A solution approach for sustainable multi-objective multi-item 4D solid transportation problem involving triangular intuitionistic fuzzy parameters*, J. Clean. Prod. **414** (2023) 137661.

[15] A.K. Bind, D. Rani, A. Ebrahimnejad, J.L. Verdegay, *New strategy for solving multi-objective green four dimensional transportation problems under normal type-2 uncertain environment*, Eng. Appl. Artif. Intell. **137** (2024) 109084.

[16] S. Biswas, K. Mishra, U.K. Bera, *Soft computing-enabled optimization of multi-choice stochastic transportation problem involving exponential and logistic distributions*, Proc. Natl. Acad. Sci. India Sect. A Phys. Sci. **96** (2026) 341-356.

Corrected Proof

[17] A.K. Bit, M.P. Biswal, S.S. Alam, *Fuzzy programming approach to multiobjective solid transportation problem*, Fuzzy Sets Syst. **57** (1993) 183-194.

[18] T.K. Buvaneshwari, D. Anuradha, *Solving bi-objective bi-item solid transportation problem with fuzzy stochastic constraints involving normal distribution*, AIMS Math. **8** (2023) 21700-21731.

[19] B. Chaini, N. Ranarahu, *Type-2 fuzzy stochastic transportation problem with gamma distribution*, Int. J. Fuzzy Log. Intell. Syst. **23** (2023) 91-105.

[20] S. Chen, *Solving Static and Dynamic Stochastic Optimization Problem via Sparse Grid and Interior Point Methods and Complexity Analysis*, Ph.D. Thesis, Northwestern University, Evanston, IL, 2008.

[21] L. Cooper, L.J. Leblanc, *Stochastic transportation problems and other network related convex problems*, Nav. Res. Logist. Q. **24** (1977) 327-337.

[22] G.B. Dantzig, *Linear Programming and Extensions*, Princeton University Press, Princeton, NJ, 1963.

[23] S.K. Das, F.Y. Vincent, S.K. Roy, G.W. Weber, *Location-allocation problem for green efficient two-stage vehicle-based logistics system: A type-2 neutrosophic multi-objective modeling approach*, Expert Syst. Appl. **238** (2024) 122174.

[24] K. Deb, S. Agrawal, A. Pratap, T. Meyarivan, *A fast elitist non-dominated sorting genetic algorithm for multi-objective optimization: NSGA-II*, in: Parallel Problem Solving from Nature PPSN VI, Springer, Berlin, 2000, pp. 849-858.

[25] K. Deb, *Multi-objective optimisation using evolutionary algorithms: an introduction*, in: Multi-Objective Evolutionary Optimisation for Product Design and Manufacturing, Springer, London, 2011, pp. 3-34.

[26] S. Devnath, M. De, S.S. Mondal, M. Maiti, *Two-stage multi-item 4-dimensional transportation problem with fuzzy risk and substitution*, J. Ambient Intell. Humaniz. Comput. **14** (2023) 9469-9496.

[27] A. Dhanapal, N.D. Devarajan, E. Kumar, *A two-stage framework for bi-objective fixed charge 4-dimensional fractional transportation problem with stochastic constraints*, J. Dyn. Games **12** (2025) 1-24.

[28] W. Ding, J. Liu, W. Dong, F. Luo, C. Gu, *MPCMO: An improved multi-population co-evolutionary algorithm for many-objective optimization*, Inf. Sci. **712** (2025) 122671.

[29] A.A. Gessesse, R. Mishra, *Multi-objective linear fractional stochastic transportation problems involving logistic distribution*, in: Lecture Notes in Electrical Engineering, Springer, Singapore, 2021, pp. 1-12.

[30] S. Ghosh, S.K. Roy, A. Ebrahimnejad, J.L. Verdegay, *Multi-objective fully intuitionistic fuzzy fixed-charge solid transportation problem*, Complex Intell. Syst. **7** (2021) 1009-1023.

Corrected Proof

[31] S. Ghosh, S.K. Roy, J.L. Verdegay, *Fixed-charge solid transportation problem with budget constraints based on carbon emission in neutrosophic environment*, Soft Comput. **26** (2022) 11611-11625.

[32] P.K. Giri, M.K. Maiti, M. Maiti, *Fuzzy stochastic solid transportation problem using fuzzy goal programming approach*, Comput. Ind. Eng. **72** (2014) 160-168.

[33] P. Grzegorzewski, *The Hamming distance between intuitionistic fuzzy sets*, in: Proceedings of the 10th IFSA World Congress, IFSA, Istanbul, 2003, pp. 35-38.

[34] F.L. Hitchcock, *The distribution of a product from several sources to numerous localities*, J. Math. Phys. **20** (1941) 224-230.

[35] J.H. Holland, *Adaptation in Natural and Artificial Systems*, The University of Michigan Press, Ann Arbor, MI, 1975.

[36] H. Jain, K. Deb, *An evolutionary many-objective optimization algorithm using reference-point based nondominated sorting approach, Part II: Handling constraints and extending to an adaptive approach*, IEEE Trans. Evol. Comput. **18** (2014) 602-622.

[37] E. Jain, J.M. Dhodiya, *Multi-objective evolutionary algorithms for solving a green multi-item fixed-charge 5D transportation problem under intuitionistic fuzzy uncertainty*, Swarm Evol. Comput. **104** (2026) 102368.

[38] V. Kakran, J. Dhodiya, *Four-dimensional uncertain multi-objective multi-item transportation problem*, Oper. Res. Decis. **32** (2022) 91-108.

[39] N. Kapoor, K.K. Paidipati, T. Ganesh, *A solution method for multi-objective fully Fermatean fuzzy transportation problems under stochastic conditions*, Oper. Res. Forum **7** (2026) 29.

[40] M.B. Kar, P. Kundu, S. Kar, T. Pal, *A multi-objective multi-item solid transportation problem with vehicle cost, volume and weight capacity under fuzzy environment*, J. Intell. Fuzzy Syst. **35** (2018) 1991-1999.

[41] C. Kar, M.S. Aktar, M. Maiti, P. Das, *Solving fully neutrosophic incompatible multi-item fixed charge four-dimensional transportation problem with volume constraints*, New Math. Nat. Comput. **20** (2024) 61-89.

[42] K. Kaspar, K. Palanivel, *Novel sustainable green transportation: A neutrosophic multi-objective model considering various factors in logistics*, Sustain. Comput. Inform. Syst. **46** (2025) 101096.

[43] B. Kaushal, R. Arora, S. Arora, *An aspect of bilevel fixed charge fractional transportation problem*, Int. J. Appl. Comput. Math. **6** (2020) 14.

[44] J. Kennedy, R. Eberhart, *Particle swarm optimization*, in: Proceedings of ICNN'95 - International Conference on Neural Networks, Vol. 4, IEEE, Piscataway, NJ, 1995, pp. 1942-1948.

[45] A. Kumar, B. Mishra, *A novel approach for solving multi-objective fuzzy-stochastic programming problem by using goal programming*, Fuzzy Inf. Eng. **18** (2026) 149-167.

Corrected Proof

[46] A. Kumar, P. Singh, *Hesitant fuzzy programming strategies for solving multi-objective neutrosophic fractional stochastic transportation problem*, Eng. Appl. Artif. Intell. **176** (2026) 114688.

[47] K. Kushwaha, R.K. Jana, P. Dutta, *Multi-objective multi-item solid transportation problem using penalty-based NSGA-II: a case-based illustration on fertilizer transportation in India*, Sādhanā **50** (2025) 67.

[48] D.R. Mahapatra, S. Panda, S.S. Sana, *Multi-choice and stochastic programming for transportation problem involved in supply of foods and medicines to hospitals with consideration of logistic distribution*, RAIRO Oper. Res. **54** (2020) 1119-1132.

[49] S. Midya, S.K. Roy, V.F. Yu, *Intuitionistic fuzzy multi-stage multi-objective fixed-charge solid transportation problem in a green supply chain*, Int. J. Mach. Learn. Cybern. **12** (2021) 699-717.

[50] D.M. Moges, A.T. Janka, B.G. Wordofa, *Hierarchical multiobjective linear fractional stochastic optimization problem under neutrosophic environment with its application in industrial production planning problems*, J. Appl. Math. **2026** (2026) 9078433.

[51] A. Mondal, S.K. Roy, S. Midya, *Intuitionistic fuzzy sustainable multi-objective multi-item multi-choice step fixed-charge solid transportation problem*, J. Ambient Intell. Humaniz. Comput. **14** (2023) 6975-6999.

[52] H.M. Nehi, H.R. Maleki, *Intuitionistic fuzzy numbers and their applications in fuzzy optimization problems*, in: Proceedings of the 9th WSEAS International Conference on Systems, WSEAS Press, Athens, 2005, pp. 1-5.

[53] D. Rani, T.R. Gulati, *Uncertain multi-objective multi-product solid transportation problems*, Sādhanā **41** (2016) 531-539.

[54] S.R. Reddy, G.S. Dulikravich, *Many-objective differential evolution optimization based on reference points: NSDE-R*, Struct. Multidiscip. Optim. **60** (2019) 1455-1473.

[55] P.K. Rout, S. Nanda, M.M. Acharya, S. Acharya, *Multi-choice multi objective fuzzy stochastic transportation problem*, Oper. Res. **66** (2026) 43-66.

[56] S.K. Roy, *Multi-choice stochastic transportation problem involving Weibull distribution*, Int. J. Oper. Res. **21** (2014) 38-58.

[57] S. Samanta, D. Chakraborty, D.K. Jana, *Uncertain 4D-transportation problem with maximum profit and minimum carbon emission*, J. Anal. **32** (2024) 471-508.

[58] S. Samanta, D. Chakraborty, D.K. Jana, *Neutrosophic multi-period two stage four-dimensional transportation problem for breakable items*, Expert Syst. Appl. **246** (2024) 123266.

[59] E. Shell, *Distribution of a product by several properties*, in: Proceedings of the Second Symposium on Linear Programming, Vol. 2, National Bureau of Standards, Washington, DC, 1955, pp. 615-642.

[60] S. Singh, A. Pradhan, M.P. Biswal, *Multi-objective solid transportation problem under stochastic environment*, Sādhanā **44** (2019) 105.

Corrected Proof

[61] J.M. Sosa, J.M. Dhodiya, *Genetic algorithm-based solution of multi-objective stochastic transportation problem*, Int. J. Adv. Oper. Manag. **13** (2021) 113-128.

[62] N. Srinivas, K. Deb, *Muiltiobjective optimization using nondominated sorting in genetic algorithms*, Evol. Comput. **2** (1994) 221-248.

[63] Y. Tang, H. Li, H. Zhang, J. Sun, *A hybrid evolutionary framework assisted by reinforcement learning for mixed multi-objective optimization features*, Appl. Soft Comput. **278** (2025) 114318.

[64] A. Todkar, J.M. Dhodiya, *Aspiration level-based non-dominated sorting genetic algorithm-II and III for multi-objective shortest path problem in a trapezoidal environment*, Int. J. Math. Oper. Res. **27** (2024) 223-253.

[65] V. Traneva, S. Tranev, *Two-stage three-dimensional transportation optimization under elliptic intuitionistic fuzzy quadruples: An index-matrix interpretation*, Axioms **14** (2025) 849.

[66] R. Verma, M.P. Biswal, A. Biswas, *Fuzzy programming technique to solve multi-objective transportation problems with some non-linear membership functions*, Fuzzy Sets Syst. **91** (1997) 37-43.

[67] A.C. Williams, *A stochastic transportation problem*, Oper. Res. **11** (1963) 759-770.

[68] L.A. Zadeh, *Fuzzy sets as a basis for a theory of possibility*, Fuzzy Sets Syst. **1** (1978) 3-28.

[69] H. Zhang, Q. Li, X. Yao, *PEAC-HNF: A novel multi-objective evolutionary algorithm for split delivery vehicle routing with three-dimensional loading constraints*, IEEE Trans. Emerg. Top. Comput. Intell. **9** (2024) 2830-2845.

[70] L. Zhang, W. Li, Y. Zheng, X. Yao, R. Wang, T. Zhang, *High-dimensional multimodal multi-objective optimization via subspace projection and angular diversity management*, Expert Syst. Appl. **316** (2026) 131814.

[71] H.-J. Zimmermann, *Fuzzy programming and linear programming with several objective functions*, Fuzzy Sets Syst. **1** (1978) 45-55.

Corrected Proof